

The Newtonian Telescope : the position and dimension of the secondary mirror in the fully illuminated field. Illumination of the field of view and vignetting. Field curvature and coma. Collimation.

Lionel Fournigault

October 2013
version project 0.9 (Capella)

Abstract

This document presents the optical system of the Newtonian telescope, and is mainly intended to amateur telescope builders as well as the users of this type of optical instrument. There are already numerous documents on the internet which deal with this subject, mostly from English sources. This document is a translation of the original written in Moliere's own language, French. It deals specifically with what we call the 'fully illuminated field', as well as the dimensioning and positioning of the elliptical secondary mirror. A spreadsheet on a single Web page using the formulae shown in this document is available at the following address :

<http://imarek.free.fr/astro/newton/newtonform-uk.php>

Contact via e-mail : lionel.fournigault@free.fr

1 Introduction.

The main aim of this document is to explain and analyse how a Newtonian telescope functions, and thus to provide useful information to the amateur users and constructors of this telescope. All the information covered has been more or less part of our knowled for a while, but not necessarily regrouped in one single document, or presented in the same way. The first part of this document deals with the dimensioning and positioning of the secondary mirror in the fully illuminated field. The second part covers the illumination of the global field of view and the vignetting. The final part covers the field curvature and coma. And, lastly, it describes the different stages in carrying out the collimation.

2 Mirrors and fully illuminated field.

The primary parabolic mirror of diameter D has a focal length marked f . These two parameters are the source data of the geometry of this problem and are considered as constants, as well as z whose value in relation to D and f , is given by the equation of the parabola, defined by its focus : $z = \frac{x^2}{2e}$ with $e = 2f$. When $x = \frac{D}{2}$ we get : $z = \frac{D^2}{16f}$ which we can express in relation to the optical focal ratio $F = \frac{f}{D}$:

$$z = \frac{D}{16F} \quad (1)$$

In the diagram 1, the fully illuminated field is represented by the segment $[KL]$ which is equal to segment $[NP]$ on the focal plane after reflection in the secondary mirror. Its dimension will be marked C_{pl} (the diameter of this field). This fully illuminated field represents a collection of points, each one of which is illuminated by the same surface of the primary mirror. This is at 100% when we don't have any obstruction of the secondary mirror. The outer incident rays marked from 1 to 4 characterise the fully illuminated field on the plane containing the respective optical axis of the 2 mirrors.

The angle α of the actual visual field, relative to this fully illuminated field, is taken away from the relation $(f - z) \tan(\alpha/2) = C_{pl}/2$ or :

$$\alpha_{pl} = 2 \arctan \frac{C_{pl}}{2 \left(f - \frac{D^2}{16f} \right)} \approx 2 \arctan \frac{C_{pl}}{2f} \quad (2)$$

The positioning of the secondary mirror, which intercepts the light cone at 45° depends on its own dimensions, on the fully illuminated field and also on the distance between it and the focal plane. These 3 parameters are marked a (minor axis), C_{pl} and p respectively. We will thus look for the relations that link a , p and C_{pl} . The obtaining of two of these parameters allows us to deduce the third. For example, if the fully illuminated field is fixed, there is an infinite number of possible solutions in accordance with the dimension of the secondary mirror and its distance p to the focal plane. The choice of p will thus provide the unique solution giving the dimension and position of the secondary mirror.

We can also see on figure 1 that the optical centre C , (the intersection of the primary and secondary mirrors's optical axis) does not correspond to the geometric centre of the secondary mirror. There is a horizontal and vertical difference of the same size marked Δ (delta) which needs to be calculated.

2.1 Approximate formulae.

When reading up on this subject, we frequently come across a relatively simple formula, given as being the dimension of the minor axis of the secondary elliptical mirror. It implies that this dimension, a' , is that of the breadth of the cone AOB on the plane containing

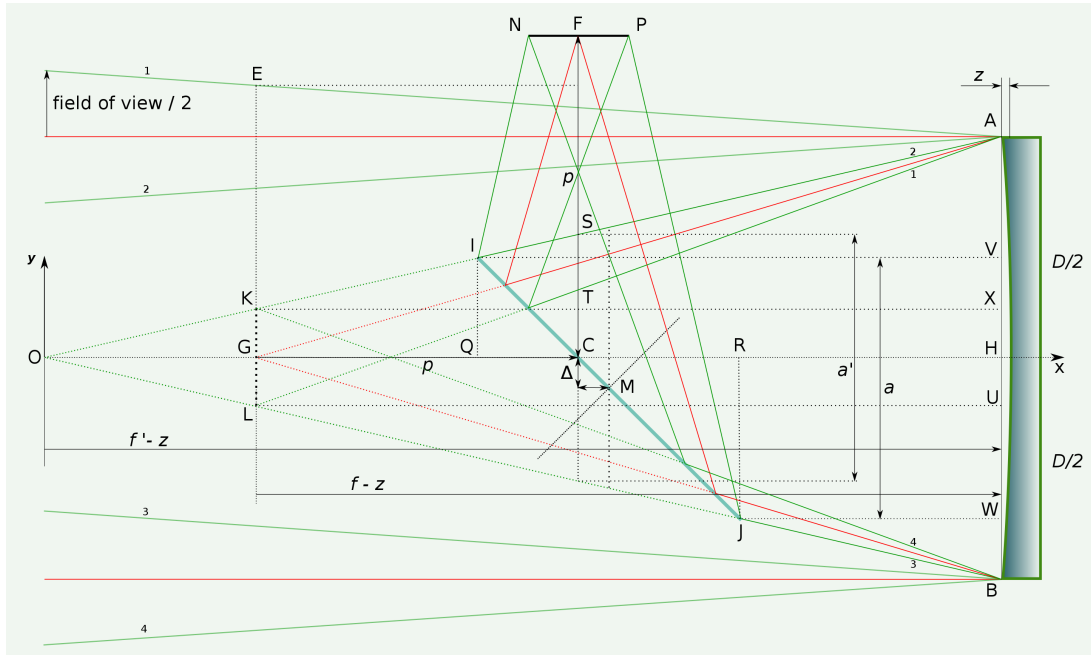


FIGURE 1 – Basic diagram of the Newtonian telescope and its fully illuminated field.

C and perpendicular to the optical axis of the primary mirror. It is calculated from the triangles KST et KAX from which we can deduce the following relations :

$$\frac{(f - z)}{AX} = \frac{p}{ST} \implies \frac{(f - z)}{\frac{D}{2} - \frac{C_{pl}}{2}} = \frac{p}{CS - \frac{C_{pl}}{2}}$$

Thus :

$$CS = \frac{p(D - C_{pl})}{2(f - z)} + \frac{C_{pl}}{2}$$

a' being equal to $2CS$, we can deduce :

$$a' = \frac{p(D - C_{pl})}{(f - \frac{D^2}{16f})} + C_{pl} \approx \frac{p(D - C_{pl})}{f} + C_{pl} \quad (3)$$

However, a' is not the dimension of the secondary mirror's minor axis, even if it does come close. This simplification would be like saying that Δ does not exist, which is by definition impossible. The simplification is thus a little excessive, but despite this, the difference between a' et a is relatively small.

The value of a , for its part, corresponds to the diameter of the cone AOB on the plane containing M and perpendicular to the optical axis of the primary mirror. The relation which connects a' and a is given by the following formula : $a = \frac{a'}{2} + \sqrt{\frac{a'^2}{4} + 4\Delta^2}$ with Δ which depends on p and a or C_{pl} (see demonstration in section 2.3.4).

It would be better to use the 4 following approximate formulae, which are approximations of exact formulae where z is small compared to f

1. If the fully illuminated field (C_{pl}) is known first, as well as p :

$$a = \frac{4f [p(D - C_{pl}) + fC_{pl}]}{4f^2 - (D - C_{pl})^2} \quad (4)$$

With a now being known :

$$\Delta = \frac{a(D - C_{pl})}{4f} \quad (5)$$

2. If the minor axis (a) of the secondary mirror is known first, as well as p :

$$\Delta = \frac{(f - p) - \sqrt{(f - p)^2 - a(D - a)}}{2} \quad (6)$$

With Δ now being known :

$$C_{pl} = \frac{af - D(p + \Delta)}{(f - p - \Delta)} \quad (7)$$

The previous formulae, which will be covered again in section 2.3, are more than enough for amateur constructors of the Newtonian telescope to get by with. Nevertheless, if the primary mirror has a small focal ratio, (for example, where $F < 4$), it would be better to use the exact, specific formulae. Still, we can keep in mind that very small differences or gaps in the positioning and dimensioning of the secondary mirror given by these formulae using theoretical values would not in fact alter the quality or the defects of the future telescope too much (at most, we would just lose a minute amount of available light energy).

2.2 The appropriate approach to take.

In the afore mentioned approximate formulae, we can see that the parameters are dependent on each other ; in order to calculate a we must first identify C_{pl} and p . But C_{pl} and p depend on a etc. To get around this problem, we can use the following approach, which is one of a selection of possibilities. It consists of three steps :

1. We first fix the dimension of the fully illuminated field C_{pl} . In order to do this, we can use the following criteria :
 - (a) Visually, the actual field of view in the eyepiece is equal to the field of view of the eyepiece divided by the magnification, which itself is equal to the ratio of the focal lengths of the primary mirror and the eyepiece. The maximum usable field of view would thus be obtained with the minimum magnification

given by the equation $G_{min} = \frac{D}{6}$ with D en mm et 6 representing the average diameter in mm of the pupil of the eye in the observation conditions. If we wish to have a fully illuminated field which is equal to this maximum field of view, its dimension will be (using the formula 2) :

$$C_{pl.max} = 2f \tan \left(\frac{Field_{eyepiece}}{2G_{min}} \right)$$

We must also ensure that there is minimal obstruction of the primary mirror by the secondary mirror, in order to capture as much light as possible. A slight loss of contrast can also be noticed when this obstruction increases, particularly with low-contrast, faint objects such as planets. To add to all this, we can also encounter problems with vignetting (see section 3). This vignetting, on the background of a starry sky, is barely visible to the eye. The largest luminous object in the night sky is the Moon, and we can in fact fix the fully illuminated field using its angular size. This is found using the formula (2) :

$$C_{pl} = 2f \tan \frac{\alpha}{2} \quad (8)$$

With $\alpha = 0,5^\circ$ (angular diameter of the full moon), we obtain about $9mm$ per meter of focal length of the primary mirror for the dimension of the fully illuminated field. This fully illuminated field will thus be a minimum, marked $C_{pl.min}$.

- (b) Another criterion concerns the astrophotography at focal plane of the telescope, and in particular, the size of the image sensors. These can be quite varied and diverse, but it can nevertheless be feasible to fix the dimension of the fully illuminated field at a value comparable to that of the sensors (format APS-C or 24x36).

With these criteria we can see that in each case there is a compromise to be made, which is up to you to decide. However, if a more formal opinion on the dimension of the fully illuminated field must be given, let's simply give it as $C_{pl.min} + 6mm$. For the focal lengths $1m$, $2m$ or $3m$ of the primary mirror, we obtain 15 , 24 and $33mm$, respectively, for the dimension of the fully illuminated field.

2. Having obtained the dimension of the fully illuminated field (C_{pl}), we must now determine the distance from the focal plane to the secondary mirror, and thus fix the measurement of p . This is the most delicate part of the calculations, as it depends on a minimum strength of the focuser, and on the different possible optical combinations that we decide to use at focal plane (various eyepieces, Barlow lens, cameras, CCDs, filter wheels, field correctors etc).

Initially, we can find this measurement by taking the diameter of the telescope's front aperture, located in this case on the same plane as the virtual focal plane

and which has the dimension $D + C_{pl}$ (figure 1). This dimension, which is the interior diameter of the tube, must be increased according to the desired level of illumination of the edge of the visual field (see section 3). This is the reason why it is necessary to add a certain margin to the measurement of p . Don't forget the thickness of the tube to be used. Having obtained p , we can now calculate the dimension of the secondary mirror's minor axis, as well as Δ by using the formulae (4) et (5).

3. We now have our correctly-dimensioned secondary mirror, in which case all its parameters have been calculated and obtained. If this isn't the case, it is thus necessary to recalculate Δ and C_{pl} . with the formulae (6) and (7). We assume here that the secondary mirror has been manufactured at the correct dimension, or that it has been bought in the shops, with a dimension as close as possible to that calculated previously.

2.3 The exact formulae.

The following exercise isn't really of any practical interest if it isn't to show from where the approximate formulae came, the answer to which doesn't exactly fall from the sky, even a starry one! However, let's not exclude any amateur Newtonian telescope builders who indeed do wish to dimension and position their secondary mirror extremely precisely, or those who have a primary mirror with a low focal ratio and whose dimension of z is no longer negligible compared to f .

To carry out these calculations, there are two methods : one is geometric and the other analytic. These will both be explained. What we use here are essentially Thales' theorem and the solution of quadratic equations.

2.3.1 Preliminary calculations.

We take $F = \frac{f}{D}$ and $F' = \frac{f'}{D}$. From the triangles OGK et KXA we can deduce OG :

$$\frac{OG}{GK} = \frac{KX}{XA} \iff \frac{OG}{\frac{C_{pl}}{2}} = \frac{(f-z)}{\frac{D}{2} - \frac{C_{pl}}{2}} \iff OG = C_{pl} \frac{(f-z)}{(D-C_{pl})}$$

Either by replacing z by $\frac{D}{16F}$ or $\frac{D^2}{16f}$

$$OG = C_{pl} D \frac{\left(F - \frac{1}{16F}\right)}{(D - C_{pl})} \text{ or } OG = C_{pl} \frac{\left(f - \frac{D^2}{16f}\right)}{(D - C_{pl})} \quad (9)$$

We can now deduce F' :

$$F' = \frac{f'}{D} = \frac{f + OG}{D} = F + C_{pl} \frac{\left(F - \frac{1}{16F}\right)}{(D - C_{pl})}$$

Thus :

$$F' = \frac{\left(f - \frac{C_{pl}D}{16f}\right)}{(D - C_{pl})} \quad (10)$$

F' characterises the light cone delimited by the primary mirror with a focal ratio $F = \frac{f}{D}$ and by the fully illuminated field C_{pl} . When $C_{pl} = 0$ we find that $F' = F$.

For the analytical method, we just need to refer to the Cartesian coordinate system xOy and use the straight line equations, which support, respectively, the segments $[OA]$ and $[OB]$ of the light cone, with the one supporting the segment $[IJ]$ representing the secondary mirror. They are easily identifiable, and are of the type $y = ax + b$:

$$y_{oa} = \frac{Dx}{2(f' - z)} \quad y_{ob} = \frac{-Dx}{2(f' - z)} \quad y_{ij} = -x + (OG + p)$$

2.3.2 Calculation of a and Δ if C_{pl} and p have been obtained first.

1. Geometric method.

From the triangles KAX and LUB we have :

$$\frac{p - \text{QC}}{\text{QI} - \frac{C_{pl}}{2}} = \frac{f - z}{\frac{D}{2} - \frac{C_{pl}}{2}}$$

With $\text{QI}=\text{QC}$ by construction we can easily deduce QC :

$$\text{QC} = \frac{p(D - C_{pl}) + C_{pl}(f - z)}{2(f - z) + (D - C_{pl})}$$

Likewise

$$\frac{p + \text{RC}}{\text{RJ} - \frac{C_{pl}}{2}} = \frac{f - z}{\frac{D}{2} - \frac{C_{pl}}{2}}$$

With $\text{RJ}=\text{RC}$ by construction we can easily deduce RC :

$$\text{RC} = \frac{p(D - C_{pl}) + C_{pl}(f - z)}{2(f - z) - (D - C_{pl})}$$

We can now write $a = \text{QC} + \text{RC}$:

$$a = \left[\frac{p(D - C_{pl}) + C_{pl}(f - z)}{2(f - z) + (D - C_{pl})} \right] + \left[\frac{p(D - C_{pl}) + C_{pl}(f - z)}{2(f - z) - (D - C_{pl})} \right]$$

Finally :

$$a = \frac{4 \left(f - \frac{D^2}{16f}\right) \left[p(D - C_{pl}) + C_{pl} \left(f - \frac{D^2}{16f}\right)\right]}{\left[2 \left(f - \frac{D^2}{16f}\right) + (D - C_{pl})\right] \left[2 \left(f - \frac{D^2}{16f}\right) - (D - C_{pl})\right]} \quad (11)$$

If we disregard the term $\frac{D^2}{16f}$ which is small compared to f we can find the approximate formula given in (4).

On the other hand, we have $RC - QC = 2\Delta$ that is :

$$\Delta = \frac{1}{2} \left[\frac{p(D - C_{pl}) + C_{pl}(f - z)}{2(f - z) - (D - C_{pl})} - \frac{p(D - C_{pl}) + C_{pl}(f - z)}{2(f - z) + (D - C_{pl})} \right]$$

And finally by replacing z by $\frac{D^2}{16f}$:

$$\Delta = \frac{(D - C_{pl}) \left[p(D - C_{pl}) + C_{pl} \left(f - \frac{D^2}{16f} \right) \right]}{\left[2 \left(f - \frac{D^2}{16f} \right) - (D - C_{pl}) \right] \left[2 \left(f - \frac{D^2}{16f} \right) + (D - C_{pl}) \right]}$$

We can shorten this previous equation by noting that the denominator and the second factor of the numerator are respectively identical to those of a (11), we thus obtain :

$$\Delta = \frac{a(D - C_{pl})4f}{16f^2 - D^2} \quad (12)$$

So now we can calculate Δ with this formula, once a is obtained. If we disregard the term D^2 which is small compared to $16f^2$ we can successfully find the approximate formula given in (5). We can also calculate delta in another way, using the triangles OIQ, OAH, OJR and OHB from which we can deduce the following relations :

$$\frac{QI}{OQ} = \frac{\frac{D}{2}}{f' - z} \quad \text{and} \quad \frac{RJ}{OR} = \frac{\frac{D}{2}}{f' - z}$$

Given that $QI=QC$ and $RJ=RC$, and replacing z with $\frac{D}{16F}$ and f' with $F'D$:

$$\frac{QC}{OQ} = \frac{\frac{D}{2}}{F'D - \frac{D}{16F}} \quad \text{and} \quad \frac{RC}{OR} = \frac{\frac{D}{2}}{F'D - \frac{D}{16F}}$$

Thus :

$$OQ = 2QC \left(F' - \frac{1}{16F} \right) \quad \text{and} \quad OR = 2RC \left(F' - \frac{1}{16F} \right)$$

On one hand, we know that $OR - OQ = a$ and on the other hand that $QC = \frac{a}{2} - \Delta$ and $RC = \frac{a}{2} + \Delta$, we can thus write :

$$a = 2 \left(F' - \frac{1}{16F} \right) (RC - QC)$$

And so :

$$a = 2 \left(F' - \frac{1}{16F} \right) \left[\left(\frac{a}{2} + \Delta \right) - \left(\frac{a}{2} - \Delta \right) \right]$$

We can obtain delta using F and F' :

$$\Delta = \frac{a}{4 \left(F' - \frac{1}{16F} \right)}$$

And by replacing F' by its expression in (10) and F by $\frac{f}{D}$:

$$\Delta = \frac{a}{4 \left[\frac{\left(f - \frac{C_{pl}D}{16f} \right)}{(D - C_{pl})} - \frac{D}{16f} \right]}$$

Finally :

$$\Delta = \frac{a(D - C_{pl})4f}{16f^2 - D^2}$$

2. Analytical method.

In the Cartesian coordinate system xOy , the coordinates x_i and x_j relative to points I and J are given by the solutions of the identities $y_{oa} = y_{ij}$ and $y_{ob} = y_{ij}$ so :

$$\frac{Dx}{2(f' - z)} = -x + (OG + p) \quad \text{and} \quad \frac{-Dx}{2(f' - z)} = -x + (OG + p)$$

From this we deduce x_i and x_j :

$$x_i = \frac{(OG + p)}{1 + \frac{D}{2(f' - z)}} \quad x_j = \frac{(OG + p)}{1 - \frac{D}{2(f' - z)}}$$

Then $a = x_j - x_i$:

$$a = (OG + p) \left[\frac{1}{1 - \frac{D}{2(f' - z)}} - \frac{1}{1 + \frac{D}{2(f' - z)}} \right]$$

So

$$a = 2(f' - z)(OG + p) \left[\frac{1}{(2(f' - z) - D)} - \frac{1}{(2(f' - z) + D)} \right]$$

Or by replacing f' by $f + OG$:

$$a = \frac{4D(OG + p)(f + OG - z)}{(2(f + OG - z) - D)(2(f + OG - z) + D)}$$

And OG by its expression in (9)

$$a = \frac{4D \left[C_{pl} \frac{(f-z)}{(D-C_{pl})} + p \right] \left[f + C_{pl} \frac{(f-z)}{(D-C_{pl})} - z \right]}{\left[2 \left(f + C_{pl} \frac{(f-z)}{(D-C_{pl})} - z \right) - D \right] \left[2 \left(f + C_{pl} \frac{(f-z)}{(D-C_{pl})} - z \right) + D \right]}$$

By multiplying top and bottom by $(D - C_{pl})$ and factorising :

$$a = \frac{4D [C_{pl}(f-z) + p(D - C_{pl})] [D(f-z)]}{[2D(f-z) - D(D - C_{pl})] [2D(f-z) + D(D - C_{pl})]}$$

So :

$$a = \frac{4(f-z) [C_{pl}(f-z) + p(D - C_{pl})]}{[2(f-z) - (D - C_{pl})] [2(f-z) + (D - C_{pl})]}$$

We end up finding the same equation, after having replaced z by its value $\frac{D^2}{16f}$, and that found in (11) with the geometric method. The coordinates x_i and x_j also allow us to calculate Δ using the following identities :

$$\text{QC} = (\text{OG} + p) - x_i \text{ et } \text{RC} = x_j - (\text{OG} + p)$$

We know that $\text{RC} - \text{QC} = 2\Delta$, we can thus deduce Δ :

$$\Delta = \frac{1}{2} [x_i + x_j - 2(\text{OG} + p)]$$

Thus :

$$\Delta = \frac{1}{2} \left[\frac{(\text{OG} + p)}{1 + \frac{D}{2(f'-z)}} + \frac{(\text{OG} + p)}{1 - \frac{D}{2(f'-z)}} - 2(\text{OG} + p) \right]$$

And by replacing f' by $f + \text{OG}$:

$$\Delta = \frac{(\text{OG} + p)}{2} \left[\frac{2(f + \text{OG} - z)}{(2(f + \text{OG} - z) + D)} + \frac{2(f + \text{OG} - z)}{(2(f + \text{OG} - z) - D)} - 2 \right]$$

And by replacing OG by its expression in (9)

$$\Delta = \frac{\left[C_{pl} \frac{(f-z)}{(D-C_{pl})} + p \right]}{2} \left[\frac{2 \left(f + C_{pl} \frac{(f-z)}{(D-C_{pl})} - z \right)}{\left[2 \left(f + C_{pl} \frac{(f-z)}{(D-C_{pl})} - z \right) + D \right]} + \frac{2 \left(f + C_{pl} \frac{(f-z)}{(D-C_{pl})} - z \right)}{\left[2 \left(f + C_{pl} \frac{(f-z)}{(D-C_{pl})} - z \right) - D \right]} - 2 \right]$$

We can thus shorten the equation by multiplying all the terms by $(D - C_{pl})$:

$$\Delta = \left[\frac{C_{pl}(f-z) + p(D - C_{pl})}{(D - C_{pl})} \right] \left[\frac{D^2(D - C_{pl})^2}{[2D(f-z) + D(D - C_{pl})][2D(f-z) - D(D - C_{pl})]} \right]$$

So finally :

$$\Delta = \frac{(D - C_{pl})[C_{pl}(f - z) + p(D - C_{pl})]}{[2(f - z) + (D - C_{pl})][2(f - z) - (D - C_{pl})]}$$

We successfully find the same equation, after having replaced z by its value $\frac{D^2}{16f}$, that found in (12) before the reduction.

The analytical method, although elegant, is less simple especially if we cannot see the possible reductions

2.3.3 Calculation of Δ and C_{pl} if the minor axis of the secondary mirror, and p , are obtained first.

With the triangles JBW and IAV, we can deduce the following relations :

$$\frac{JW}{WB} = \frac{IV}{AV} \text{ thus } \frac{f - z - p - (\frac{a}{2} + \Delta)}{\frac{D}{2} - (\frac{a}{2} + \Delta)} = \frac{f - z - p + (\frac{a}{2} - \Delta)}{\frac{D}{2} - (\frac{a}{2} - \Delta)}$$

And we obtain a simple quadratic equation :

$$\Delta^2 - \Delta(f - z - p) + \frac{a}{4}(D - a) = 0$$

which produces one solution compatible with the given problem. After having replaced z by its value $\frac{D^2}{16f}$ we can deduce Δ :

$$\Delta = \frac{(f - \frac{D^2}{16f} - p) - \sqrt{(f - \frac{D^2}{16f} - p)^2 - a(D - a)}}{2} \quad (13)$$

The other solution would place the secondary mirror well outside of the telescope itself. If we disregard the term $\frac{D^2}{16f}$ which is small relative to f we find the approximate formula (6) given in section (2.1).

From the triangle KXA and now having obtained Δ we have the following relation :

$$\frac{p + \Delta}{\frac{a}{2} - \frac{C_{pl}}{2}} = \frac{f - z}{\frac{D}{2} - \frac{C_{pl}}{2}}$$

Thus :

$$(D - C_{pl})(p + \Delta) = (f - z)(a - C_{pl})$$

And after having replaced z by its value $\frac{D^2}{16f}$, we finally obtain :

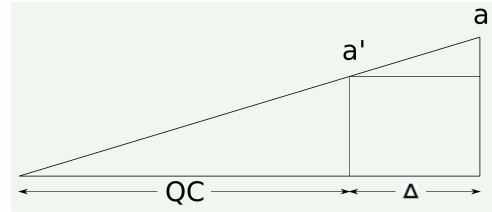
$$C_{pl} = \frac{a \left(f - \frac{D^2}{16f} \right) - D(p + \Delta)}{f - \frac{D^2}{16f} - p - \Delta} \quad (14)$$

If we disregard the term $\frac{D^2}{16f}$ which is small relative to f we can find the approximate formula (7) given in section (2.1).

2.3.4 Difference between a and a' .

The relation which exists between the diameter of cone OAB on the plane passing through C (a') and that in the plane passing through M (a) can be easily formulated. With the following identities : $QC = \frac{a}{2} - \Delta$ and

$$\frac{QC}{\frac{a'}{2} - QC} = \frac{QC + \Delta}{\frac{a}{2} - QC}$$



We can deduce the equation $a^2 - aa' - 4\Delta^2 = 0$ which produces a single solution > 0 :

FIGURE 2 – Difference between a and a' .

$$a = \frac{a'}{2} + \sqrt{\frac{a'^2}{4} + 4\Delta^2}$$

2.3.5 Numerical application.

D (primary mirror)	200 mm	300 mm	600 mm	800 mm	1000 mm
focale ($F = 5$)	1000 mm	1500 mm	3000 mm	4000 mm	5000 mm
C_{pl}	9 mm	14 mm	27 mm	36 mm	45 mm
$p = D/2 + 150$	250 mm	300 mm	450 mm	550 mm	650 mm
a' exact value	56,86 mm	71,34 mm	113,16 mm	141,31 mm	169,46 mm
a exact value	57,39 mm	72,00 mm	114,21 mm	142,62 mm	171,02 mm
a approximate value	57,27 mm	71,85 mm	113,98 mm	142,34 mm	170,70 mm
$a - a'$ exact value	0,52 mm	0,65 mm	1,04 mm	1,30 mm	1,56 mm
Δ exact value	2,74 mm	3,44 mm	5,46 mm	6,82 mm	8,18 mm
Δ approximate value	2,73 mm	3,42 mm	5,44 mm	6,79 mm	8,15 mm

D (primary mirror)	200 mm	300 mm	600 mm	800 mm	1000 mm
focale ($F = 4$)	800 mm	1200 mm	2400 mm	3200 mm	4000 mm
C_{pl}	7 mm	11 mm	22 mm	29 mm	36 mm
$p = D/2 + 150$	250 mm	300 mm	450 mm	550 mm	650 mm
a' exact value	67,54 mm	83,53 mm	130,8 mm	162,03 mm	193,26 mm
a exact value	68,55 mm	84,77 mm	132,73 mm	164,44 mm	196,13 mm
a approximate value	68,30 mm	84,47 mm	132,29 mm	163,89 mm	195,48 mm
$a - a'$ exact value	1,00 mm	1,23 mm	1,93 mm	2,40 mm	2,87 mm
Δ exact value	4,15 mm	5,12 mm	8,02 mm	9,94 mm	11,86 mm
Δ approximate value	4,11 mm	5,08 mm	7,96 mm	9,87 mm	11,77 mm

The selection of examples shown in the above table show that the differences between the exact and approximate values of Δ , and of a are in fact completely insignificant. Concerning a' , however, we can see that the difference with a is not really insignificant. As has been previously mentioned, and has been further shown just now, the approximate formulae are largely sufficient in themselves.

3 Illumination and vignetting.

In this section, the objective is to determine how illumination varies on the focal plane when we distance ourselves from the optical axis in order to move towards the edge of the global field of view. The overall aim of doing this is to calculate, if possible, the dimension of the telescope's front aperture as well as that of the focuser, according to the level of illumination desired for the edge of the field of view.

A point in infinity (a star) located in the actual field of view emits light in all directions, particularly towards the telescope, which receives via its circular front aperture a cylindrical luminous flux (the rays coming from a point in infinity are parallel). After reflection in the parabolic mirror, this luminous flux is by definition transformed into a light cone whose peak is the image on the focal plane of the point in infinity. The illumination here, or as our photographer friends would say, the clarity, is proportional to the surface, on the parabolic mirror, which has contributed to the creation of this light cone.

Here we don't take into account the field curvature on the focal plane. In the following diagrams, the elements are identical to those in figure (1) with a focal ratio equal to 1,68 and an obstruction on the diameter equal to 60%. These parameters are of course hypothetical, but do help to facilitate the identification of the problems. The lines are correct.

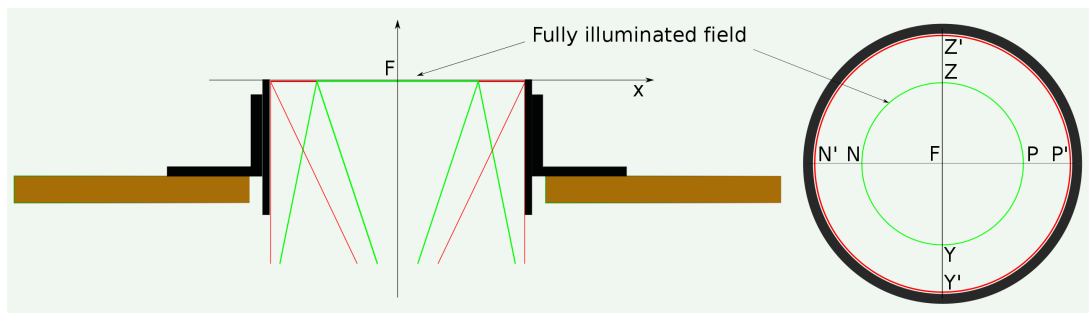


FIGURE 3 – Global field of view on the focal plane

Vignetting in a point of the field of view is when one or more elements of the telescope cut a part of the luminous flux entering, or a part of the light cone which illuminates this point. We can essentially identify 3 different types of vignetting :

1. The front aperture of the telescope on the luminous flux entering.
2. The secondary mirror on the light cone.
3. The input aperture of the focuser on the light cone.

This vignetting on the focal plane only appears outside of the fully illuminated field. It is even more important when the distance increases from the optical axis up to the edge of the global field of view. The effect is to decrease the level of illumination.

What interests us is what follows the illumination of the global field of view on the focal plane (figure 3) considering that the telescope's front aperture is dimensioned for the fully illuminated field at the distance f from the primary mirror. Concerning the dimension of the focuser's input aperture, we can assume that its value is superior or equal to the breadth of the luminous flux relative to the fully illuminated field, without vignetting. This dimension is given by the following relation, with x being the distance between the input aperture and the focal plane :

$$Pupille_{map} \geq C_{pl} + \left[x \tan \frac{\alpha}{2} \right]$$

The input aperture of the focuser being mobile, following the optical axis of the focal plane, we must be careful to dimension it without cutting off or blocking the fully illuminated field, no matter its position. In practice, unless you construct the entire system itself, the choice for the amateur constructor is limited most of the time to keeping a diameter of about 50,8mm or 76,2mm (2 or 3 inches).

3.1 Illumination of the fully illuminated field

The representation of the luminous fluxes which contribute to the illumination of each point of the fully illuminated field is not exactly an easy task. We will try it anyway for 2 particular points, P and Z which are located on the edge of the fully illuminated field (see figures 4 and 5). Here, this is a matter of looking at cross sections containing the axis of the primary mirror. A cylindrical incident flux containing an infinite number of parallel luminous rays contributes to the illumination (minus obstruction) of each point. The geometric construction is based on SNELL-DESCARTES concerning the reflection, the angle of incidence is equal to the reflected angle with respect to the surface normal and on the same plane. Here, the normal on the point of incidence on the parabolic surface is the straight line which joins this point to the centre of the curvature. In theory, the parabola has an infinite number of curvature centres, but here we can consider that the parabola being close to the circle makes this point unique, and distant from $2f$ on the axis. This approximation is enough to be able to create the lines.

In order to be able to imagine the reality a little more easily, we must try to imagine, with each figure, a rotation of incident fluxes around the direction axis (KH and YH), and imagine this added to the 3D. . .

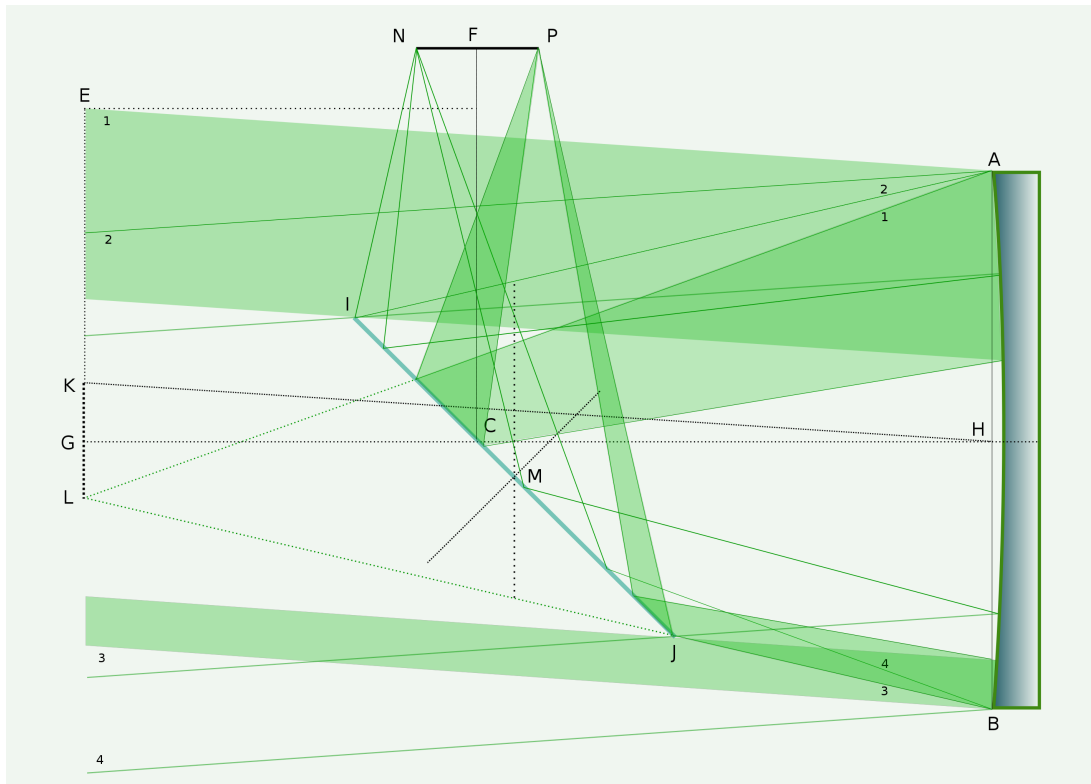


FIGURE 4 – Sectional view of illumination of point P.

After reflection in the parabolic mirror, a light cone is formed. We can here remark clearly the effect of the obstruction caused by the secondary mirror. Each light cone contains a certain volume of absence of light, this in itself also being cone-shaped. Here we've looked at 2 particular points, but the same reasoning is also applicable to the collection of points on the focal plane. For each of these points, there is a corresponding cylindrical incident flux in the direction of a point on the actual field of view and composed of an infinite number of luminous and parallel rays.

Figure 7 shows the view of the secondary mirror from the focal plane, using 3 points on the fully illuminated field, P, Z and F. By definition, all the points on the fully illuminated field are illuminated by the same surface of the primary mirror.

This would be a 100% illumination if we didn't take any obstruction into account, or if the secondary mirror was infinitely small. Each point on the fully illuminated field would thus be illuminated by the total surface of the primary mirror. The percentage of illumination, taking obstruction into account, is given simply by the following relation using the diameters of the mirrors, D and a :

$$I_{cpl} = \frac{S_{mp} - S_{oms}}{S_{mp}} = 1 - \frac{a^2}{D^2}$$

The telescope presented here, which is not realistic, would give an approximate 64% illumination of the fully illuminated field. For a classic 200/1000 commercial telescope with a 56mm secondary mirror we would obtain 92%.

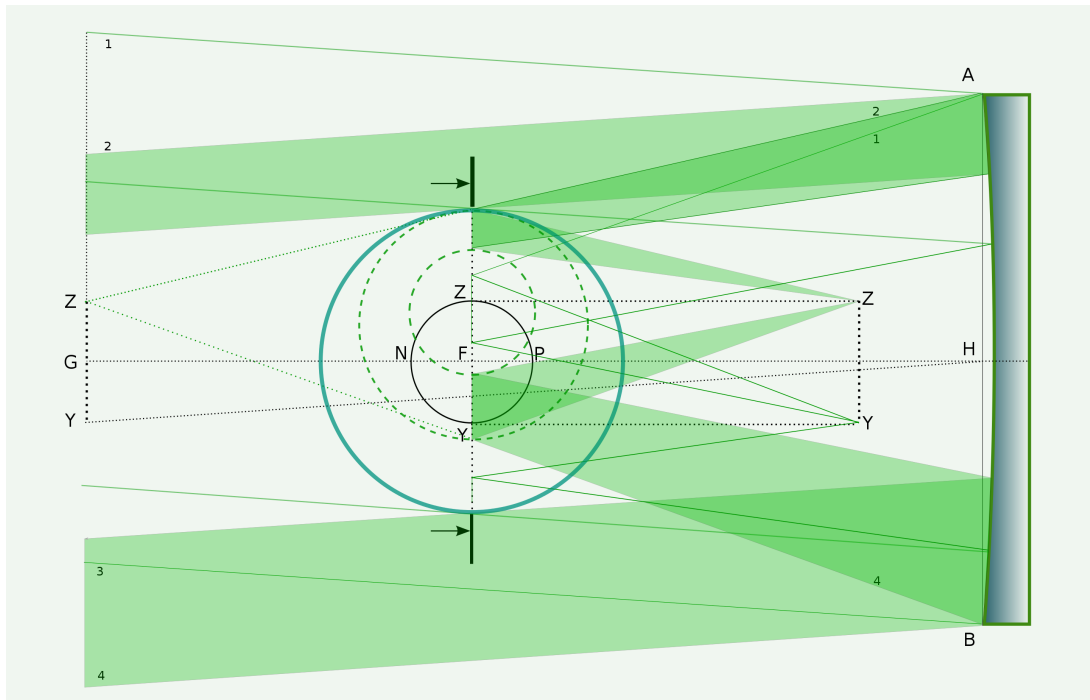


FIGURE 5 – Sectional view of the illumination of point Z.

Strictly speaking, if we take obstruction into account, the illumination in the fully illuminated field is not entirely constant. This is due to the fact that the shadow of the secondary mirror on the primary mirror is an ellipse. The parameters of this ellipse depend on the angle of the incidental rays, and so, on the distance x to the axis for the corresponding focusing point in the focal plane. This is the case for all entering luminous fluxes, except those which illuminate segment ZY on the focal plane and the one which is parallel to the primary mirror's axis. Concerning the segment PN, the illumination at a distance x from the axis is given by the following relation, which will be further explained in section 3.2.5 :

$$I_{PN}(x) = 1 - \left[\left(1 - \frac{x}{f} \right) \frac{a^2}{D^2} \right]$$

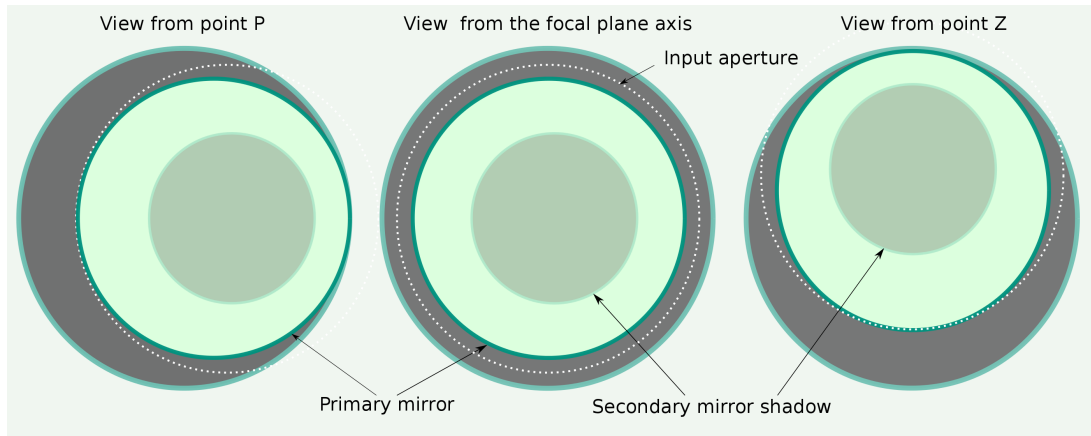


FIGURE 6 – Secondary mirror seen from points P and Z on the focal plane and from the focus.

The difference in illumination between the points P and N on the edge of the fully illuminated field, and which is symmetrical in relation to the focus, would here be about 4%. However, we are in this case using a hypothetical telescope with an unrealistic obstruction and very low focal ratio. In the case of a real telescope with a focal ratio about 4 or 5 and with an obstruction of its diameter of about 20% or 25% this difference in illumination would be minute and certainly difficult to measure. On the segment ZY, the shadow of the secondary mirror remains circular, and the illumination is thus constant.

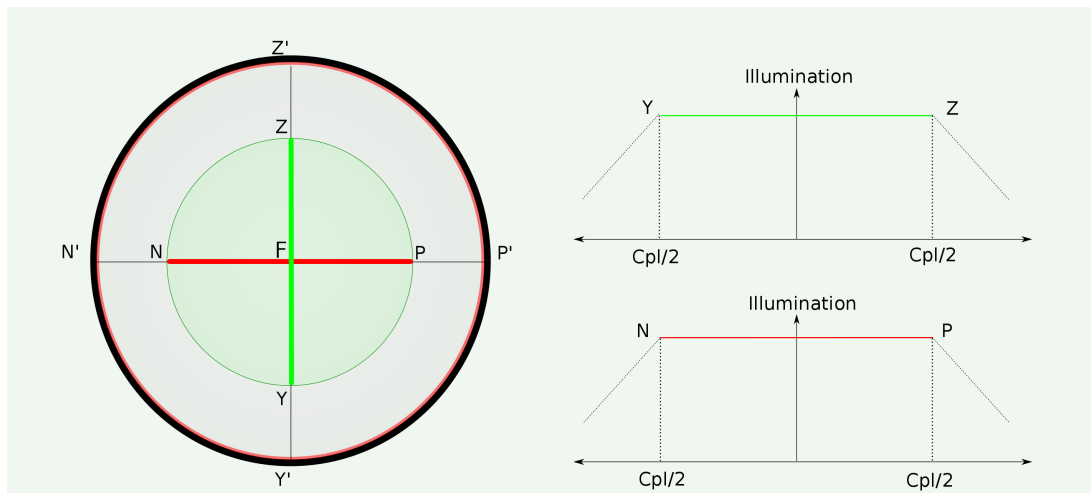


FIGURE 7 – Illumination diagram on the focal plane.

3.2 Illumination on the edge of the field of view

Here we're tackling a not-entirely trivial problem, as it consists in finding an expression representative of the illumination outside of the fully illuminated field in relation to the distance x from focal plane's axis and from all the elements of the telescope. We're looking at the zone of vignetting of one part of the light cone, which is due to the telescope's front aperture and its secondary mirror. The illumination of one point on the focal plane is proportional to the visible surface of the primary mirror which illuminates this point. We're thus looking to determine a function $I(x)$ which is connected to the 2 surfaces, one being the surface which illuminates the point at a distance x from the axis and the other being the surface which gives the maximum illumination (a totally visible primary mirror).

We'll firstly take a look at the illumination on the segment PP' of the focal plane. To do this, we'll consider an incidental luminous flux whose angle with the axis of the primary mirror is β . This flux illuminates the point x on the segment PP'. Figure 8 shows the geometry of this problem. The incidental angle β is linked to the distance x from the axis on the focal plane through the relation : $\beta = \arctan \frac{x}{f}$. We're not going to worry here about the reflection of different rays from the secondary mirror which is neutral, geometrically speaking. In order to understand this, we'll stay in the virtual focal plane on the axis of the primary mirror.

So here it's time of defining a reference plane in which we intercept the rays from the light cone, the telescope's front aperture, the secondary mirror and its shadow and everything viewed from point x . Ideally we would choose plane (P') orthogonal to the axis of the light cone, but instead we will take plane (P), the difference (around $\cos \beta$) being minimal. In the Cartesian coordinates system x'Oy', the plane (P) contains the linear equation $y = p$. Figure 9 shows the projection of these elements on the plane, seen from point x .

We first calculate all the parameters relative to the projections on plane (P) then the surfaces S1, S2 et S3 which illuminate point x .

3.2.1 Light cone

On the plane (P) the light cone is represented by points c1 et c2, intersections on the lines supporting the segments $[xA]$ et $[xB]$ with the straight line $y = p$. We deduce from this the coordinations of these points :

$$c1(x) = x - \frac{p(\frac{D}{2} + x)}{(f - z)} \text{ and } c2(x) = x + \frac{p(\frac{D}{2} - x)}{(f - z)}$$

The diameter of the light cone is simply valued $c2(x) - c1(x)$:

$$\emptyset_c = \frac{pD}{(f - z)} \text{ and the radius } R_c = \frac{pD}{2(f - z)}$$

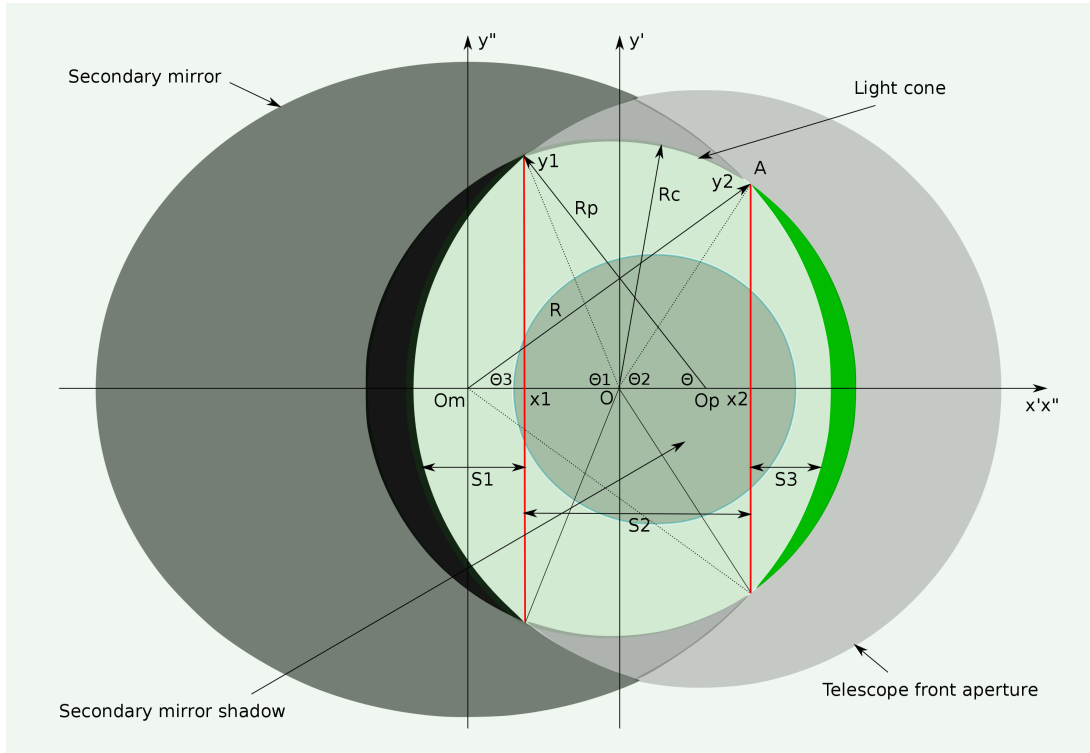


FIGURE 9 – Illumination on segment PP' in plane (P) seen from point x.

3.2.3 Secondary mirror

The projection of the secondary mirror in plane (P) can be determined analytically by considering the straight line equations which support segments $[x, a1]$ et $[x, a2]$ as well as the straight line $y = p$. In this way we can deduce the coordinates of points $m1$ et $m2$:

$$m1(x) = \frac{p[-\frac{a}{2} + \Delta - x]}{p - \frac{a}{2} + \Delta} + x \text{ and in the same way } m2(x) = \frac{p[\frac{a}{2} + \Delta - x]}{p + \frac{a}{2} + \Delta} + x$$

The diameter of the secondary mirror on axis x' is valued simply $m2 - m1$:

$$\varnothing_m(x) = \frac{pa(p+x)}{p^2 + 2\Delta p + \Delta^2 - \frac{a^2}{4}}$$

The radius on this axis thus has the value $R_m(x) = \frac{\varnothing_m(x)}{2}$ and the position of its centre in the Cartesian coordinate system $x'Oy'$ of plane (P) is :

$$O_m(x) = m2(x) - R_m(x) - (c2 - R_c)$$

We can see that the projection of the secondary mirror in plane (P) is an ellipse, whose dimension depends on the position of point x on the focal plane. When $x = 0$, in other

words at the focus, this ellipse is a circle whose diameter reaches towards a . We have here 2 parameters which define this ellipse; the small diameter which is close to a and the large diameter whose value is that previously calculated and which depends on x .

We can easily verify this when we look at the secondary mirror from the focal plane and then by moving our viewpoint either towards the primary mirror or otherwise towards the telescope's front aperture. The secondary mirror appears as an ellipse, whose own eccentricity at the focus cancels itself out.

3.2.4 Calculation of areas S1, S2 and S3

So we now have the elements which enable us to calculate the areas S1, S2 et S3 whose sum represents the visible surface of the primary mirror seen from point x on segment PP' of the focal plane. Everything we're looking at here is now taking place on plane (P) with the projections of the secondary mirror, the light cone and the telescope's front aperture (figure 9).

Regarding figure S1, we're dealing with a circular segment whose area is given through the following expression :

$$S = \frac{r^2}{2} [2\theta + \sin(2\theta)] \text{ with } R_p \cos \theta = O_p - x_1 \text{ so } \theta = \arccos \frac{O_p - x_1}{R_p}$$

Taking into account that $\sin(2 \arccos(x)) = 2x\sqrt{(1-x^2)}$ we obtain for this area :

$$S1 = R_p^2 \left[\arccos \left(\frac{O_p - x_1}{R_p} \right) - \left(\frac{O_p - x_1}{R_p} \right) \sqrt{1 - \left(\frac{O_p - x_1}{R_p} \right)^2} \right]$$

From the following relations :

$$y_1^2 + (O_p - x_1)^2 = R_p^2 \text{ and } y_1^2 + x_1^2 = R_c^2$$

We can deduce :

$$x_1 = \frac{O_p^2 - R_p^2 + R_c^2}{2O_p}$$

And by replacing R_p , R_c and O_p by their previously calculated value, we can write :

$$\frac{O_p - x_1}{R_p} = \frac{4x^2 + 2DC_{pl} + C_{pl}^2}{4x(D + C_{pl})}$$

In this expression, x is the distance to the optical axis in the focal plane. When $x = \frac{C_{pl}}{2}$ and so $\frac{O_p - x_1}{R_p} = 1$ and when $S1 = 0$, the telescope's front aperture no longer vignettes

the light cone. This means that in the focal plane, we are now on the edge of the fully illuminated field at point P.

In order to determine area $S2$ which is the sum of parts of circles and triangles, we must use the relation which gives the area of the sector of a circle :

$$S_{sector} = \frac{R^2\alpha}{2} \text{ with here } R = R_c \text{ and the value of } \alpha \text{ being either } \frac{\pi}{2} - \theta_1 \text{ or } \frac{\pi}{2} - \theta_2$$

Moreover we have :

$$R_c \cos \theta_1 = -x_1 \text{ as well as } R_c \cos \theta_2 = x_2 \text{ from which } \theta_1 = \arccos \frac{-x_1}{R_c} \text{ and } \theta_2 = \arccos \frac{x_2}{R_c}$$

As well as the areas of triangles x_1Oy_1 and x_2Oy_2 , which we must then add. The figure being symmetrical in relation to the axis of x' a factor 2 intervenes. In the end we obtain the expression giving the area $S2$:

$$S2 = R_c^2 \left[\pi - \arccos \left(\frac{-x_1}{R_c} \right) - \arccos \left(\frac{x_2}{R_c} \right) \right] - x_1 \sqrt{R_c^2 - x_1^2} + x_2 \sqrt{R_c^2 - x_2^2}$$

And finally :

$$S2 = R_c^2 \left[\pi - \arccos \left(\frac{-x_1}{R_c} \right) - \arccos \left(\frac{x_2}{R_c} \right) + \left(\frac{-x_1}{R_c} \right) \sqrt{1 - \left(\frac{-x_1}{R_c} \right)^2} + \left(\frac{x_2}{R_c} \right) \sqrt{1 - \left(\frac{x_2}{R_c} \right)^2} \right]$$

In this expression, x_1 is always < 0 and x_2 always > 0 . When $x_1 = -R_c$ and $x_2 = R_c$ we successfully obtain $S2 = R_c^2\pi$. We are here in the situation where x on the focal plane is worth $\frac{C_{pl}}{2}$, thus at point P where the vignetting has disappeared. The projection of the light cone in plane (P) is thus a non-vignetted circle.

We can verify this by replacing x_1 by its expression in relation to x , D and C_{pl} :

$$\frac{-x_1}{R_c} = \frac{-O_p^2 + R_p^2 - R_c^2}{2O_p R_c} = \frac{-4x^2 + 2DC_{pl} + C_{pl}^2}{4xD}$$

$$x = \frac{C_{pl}}{2} \implies \frac{-x_1}{R_c} = 1$$

In order to calculate x_2 , we must take into account that point A is found simultaneously on a circle with a radius R_c and on an ellipse whose axes have the values : $\emptyset_m(x)$ and $\emptyset_m(0)$. These values represent the diameters of the projection of the secondary mirror in plane (P) seen from point x in the focal plane. When $x = 0$, we are at the focus and these two values are equal.

We must therefore solve the following system, which is defined by the Cartesian equations belonging to the circle and the ellipse, but which in the Cartesian coordinate system of the ellipse : $x''Oy''$ with $x'' = x_2 - O_m(x)$

$$\begin{aligned} R_c^2 &= [x'' + O_m(x)]^2 + y_2''^2 \\ \frac{4x''^2}{\emptyset_m^2(x)} + \frac{4y_2''^2}{\emptyset_m^2(0)} &= 1 \end{aligned}$$

In setting down $u = \frac{\emptyset_m^2(0)}{\emptyset_m^2(x)}$ we obtain the quadratic equation :

$$x''^2(1 - u) + 2x''O_m(x) + O_m^2(x) - R_c^2 + \frac{\emptyset_m^2(0)}{4} = 0$$

With a positive root compatible with the data of the problem, and from which we deduce x_2 :

$$x_2 = \frac{-2O_m(x) - \sqrt{[2O_m(x)]^2 - 4(1 - u) \left[\frac{\emptyset_m^2(0)}{4} - R_c^2 + O_m^2(x) \right]}}{2(1 - u)} + O_m(x)$$

When on the focal plane, $x = \frac{C_{pt}}{2}$, we can show that $x_2 = R_c$ and $y_2 = 0$.

We can now at last determine area S_3 , which is a segment of the ellipse. We do this by using the integral which enables us to calculate the surface of half an ellipse :

$$A = ab \int_0^u \frac{1 - \cos(2u)}{2} du = ab \left[\frac{u}{2} \right]_0^u - ab \left[\frac{\sin(2u)}{4} \right]_0^u$$

When u varies from 0 to $\frac{\pi}{2}$ we can deduce the quarter of the area of an ellipse $\frac{ab\pi}{4}$. Regarding the segment of the ellipse which is here what we're interested in finding, we have :

$$x' = a \cos(u) \text{ with } x' = (x_2 - O_m(x)) \text{ then } u = \arccos \left[\frac{2(x_2 - O_m(x))}{\emptyset_m(x)} \right]$$

$$\text{As well as } a = \frac{\emptyset_m(x)}{2} \text{ and } b = \frac{\emptyset_m(0)}{2}$$

We can now write the expression of the area of segment S_3 without forgetting the factor 2 which intervenes, the figure being symmetrical in relation to the axis of x' . We also reencounter here the classic relation :

$$\sin(2 \arccos(\alpha)) = 2\alpha\sqrt{1 - \alpha^2}$$

$$S3 = \frac{1}{4} \emptyset_m(0) \emptyset_m(x) \left[\arccos \left(\frac{2(x_2 - Om(x))}{\emptyset_m(x)} \right) - \frac{2(x_2 - Om(x))}{\emptyset_m(x)} \sqrt{1 - \left(\frac{2(x_2 - Om(x))}{\emptyset_m(x)} \right)^2} \right]$$

When $x = \frac{C_{pl}}{2}$, we find ourselves at the edge of the fully illuminated field at point P, with $x_2 - Om(x) = \frac{\emptyset_m(x)}{2}$ and we can confirm $S3 = 0$. In this case, the secondary mirror covers the entirety of the light cone.

3.2.5 Shadow of the secondary mirror

It remains to determine the parameters of the projection of the secondary mirror's shadow in plane (P). To do this, we need to find the coordinates of points O_1 and O_2 which are the intersections of the straight lines of type $ax + b$, supporting segments $[xs1]$ et $[xs2]$, and with the straight line $y = p$. We obtain the following relations :

$$O_1 = -\frac{p(x - s1)}{f - z} + x \text{ as well as } O_2 = -\frac{p(x - s2)}{f - z} + x$$

Taking into account that :

$$s1 = -\left(\frac{a}{2} - \Delta\right) + \left[f - p + \frac{a}{2} - \Delta\right] \frac{x}{f}$$

$$s2 = \left(\frac{a}{2} + \Delta\right) + \left[f - p - \left(\frac{a}{2} + \Delta\right)\right] \frac{x}{f}$$

We deduce from this the diameter $O_2 - O_1$ in plane (P) :

$$\emptyset_{oms}(x) = \frac{pa \left(1 - \frac{x}{f}\right)}{f - z} \text{ as well as the surface } S_{oms}(x) = \left(1 - \frac{x}{f}\right) \left[\frac{pa}{2(f - z)}\right]^2 \pi$$

The projection of the secondary mirror's shadow in plane (P) is an ellipse, whose parameters depend on the distance x to the optical axis in the focal plane. At the focus, $x = 0$, we obtain in plane (P) a circle whose area is :

$$S_{oms}(0) = \left[\frac{pa}{2(f - z)}\right]^2 \pi$$

3.2.6 The formula...

So we now have all the necessary elements in order to express the area of the mirror which illuminates a point on the focal plane at a distance x from the axis on segment PP' . In comparing this area to that obtained when we are on the axis at the focus, we can deduce how the illumination varies in this focal plane and outside of the fully illuminated field. The ratio of these areas is a number without dimensions less than or equal to 1 depending on whether or not we take obstruction into account. We thus obtain the maximum illumination in the fully illuminated field, then a function which gradually decreases when we move away from the optical axis. The following formula remains valid when $x_1 < 0$ and $x_2 > 0$. It is defined for $x \geq \frac{C_{pl}}{2}$:

$$I_{PP'}(x) = \frac{S1(x) + S2(x) + S3(x) - S_{oms}(x)}{S2(0)} \quad (15)$$

With :

$$\begin{aligned} S1(x) &= A^2 \left[\arccos(B) - B\sqrt{1-B^2} \right] \\ S2(x) &= C^2 \left[\pi - \arccos(E) - \arccos(L) + E\sqrt{1-E^2} + L\sqrt{1-L^2} \right] \\ S3(x) &= R \left[\arccos(V) - V\sqrt{1-V^2} \right] \\ S_{oms}(x) &= T^2\pi \\ S2(0) &= C^2\pi \end{aligned}$$

And depending on the elements of the telescope, the primary mirror of diameter D , its focal distance f and its sagitta z , the secondary mirror with minor axis a , the offset Δ , the fully illuminated field C_{pl} , the distance p from the focal plane to the axis of the primary mirror and the diameter of the telescope's front aperture Pu with a value equal to $D + C_{pl}$:

$$\begin{aligned} A &= \frac{p(D+C_{pl})}{2(f-z)} \\ B(x) &= \frac{4x^2+2DC_{pl}+C_{pl}^2}{4x(D+C_{pl})} \\ C &= \frac{pD}{2(f-z)} \\ E(x) &= \frac{-4x^2+2DC_{pl}+C_{pl}^2}{4xD} \\ \emptyset_m(x) &= \frac{pa(p+x)}{p^2+2\Delta p+\Delta^2-\frac{a^2}{4}} \\ \emptyset_m(0) &= \frac{p^2a}{p^2+2\Delta p+\Delta^2-\frac{a^2}{4}} \\ m2(x) &= \frac{p[\frac{a}{2}+\Delta-x]}{p+\frac{a}{2}+\Delta} + x \\ O_m(x) &= m2(x) - \frac{\emptyset_m(x)}{2} - \left(x + \frac{p(\frac{D}{2}-x)}{(f-z)} - C \right) \\ u(x) &= \frac{\emptyset_m^2(0)}{\emptyset_m^2(x)} \\ x_2(x) &= \frac{-2O_m(x) - \sqrt{[2O_m(x)]^2 - 4(1-u) \left[\frac{\emptyset_m^2(0)}{4} - C^2 + O_m^2(x) \right]}}{2(1-u)} + O_m(x) \end{aligned}$$

$$\begin{aligned}
L(x) &= \frac{2x_2(f-z)}{pD} \\
R(x) &= \frac{\mathcal{O}_m(0)\mathcal{O}_m(x)}{\mathcal{O}_m(x)} \\
V(x) &= \frac{2(x_2 - \mathcal{O}_m(x))}{\mathcal{O}_m(x)} \\
T(x) &= \sqrt{\left(1 - \frac{x}{f}\right) \left[\frac{pa}{2(f-z)}\right]}
\end{aligned}$$

To visualise the illumination $I_{PP'}(x)$ in relation to the distance x to the axis on segment PP' , we just need to enter this formula into a calculation program, such as, *javascript* or *php* for example². We then obtain the graphs of figures 10 and 11 with and without obstruction for 2 configurations, one being that of the hypothetical telescope presented here, and the other being that of a real telescope.

We can see that the part of the curve beyond the fully illuminated field is not linear ; the opposite would have been surprising.

We can now deduce the loss of magnitude in the part of the visual field outside the fully illuminated field on segment PP' . To do this, we are going to use NORMAN POGSON formula, which gives the apparent magnitude :

$$M = -2,5 \log_{10}(\phi)$$

with ϕ being the luminous flux received. Here, what interests us is the difference in magnitude which appears when we move away from the axis of the focal plane, from one distance to another. So we have :

$$M_1 = -2,5 \log_{10}(\phi) \text{ et } M_2 = -2,5 \log_{10}(\phi I_x)$$

From this we can deduce $M_2 - M_1$:

$$\Delta m = 2,5 \log_{10} \left(\frac{1}{I_x} \right)$$

We now take an interest in the illumination on segment NN' , the method and the parameters of the projection in plane (P) are here similar. The variables x , x_1 , x_2 , O_p et O_m change signs. Figures 12 and 13 correspond to this case.

For areas S_1 , S_2 and S_3 we thus obtain :

$$S_1 = R_p^2 \left[\arccos \left(\frac{x_1 - O_p}{R_p} \right) - \left(\frac{x_1 - O_p}{R_p} \right) \sqrt{1 - \left(\frac{x_1 - O_p}{R_p} \right)^2} \right]$$

Taking into account that :

$$R_p \cos \theta = x_1 - O_p \text{ soit } \theta = \arccos \frac{x_1 - O_p}{R_p}$$

2. This does however take a little time...

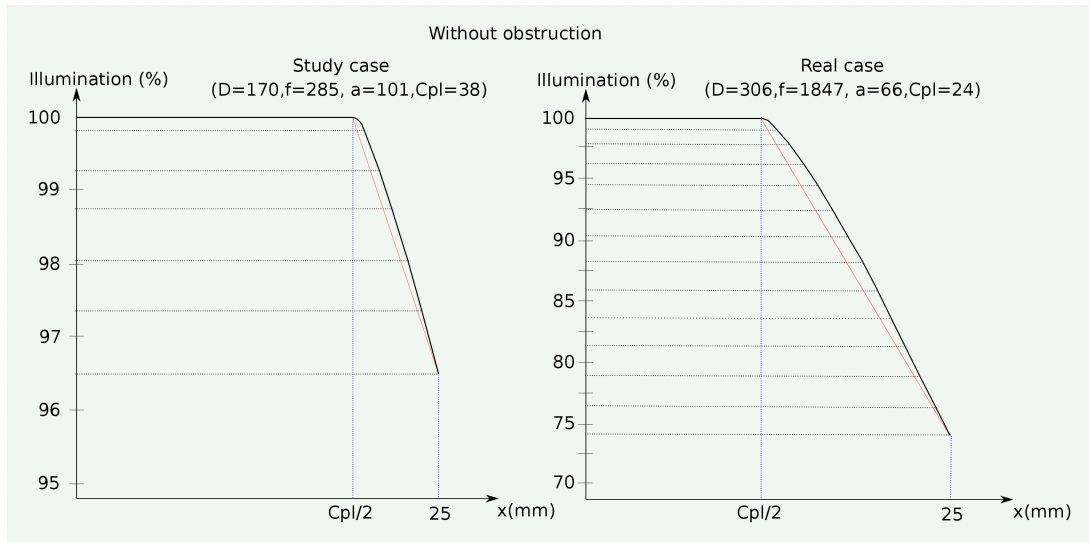


FIGURE 10 – Illumination curve on segment FP' on the focal plane, without obstruction

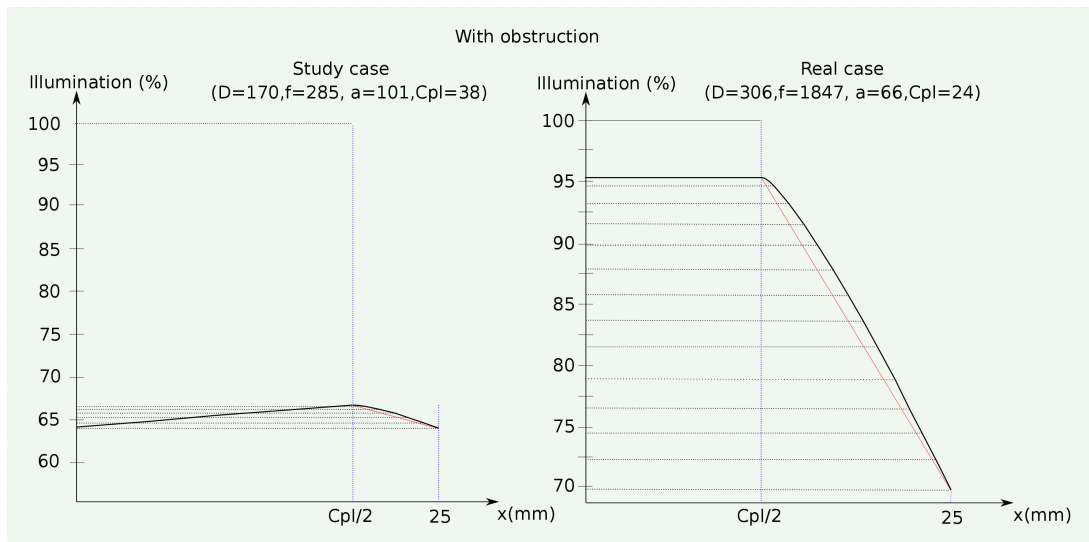


FIGURE 11 – Illumination curve on segment FP' on the focal plane, with obstruction

As well as :

$$x_1 = \frac{O_p^2 - R_p^2 + R_c^2}{2O_p} \text{ and } \frac{x_1 - O_p}{R_p} = \frac{-4x^2 - 2DC_{pl} - C_{pl}^2}{4x(D + C_{pl})}$$

When $x = -\frac{C_{pl}}{2}$, $x_1 = 1$ and $S_1 = 0$, so we are here at point N on the edge of the fully illuminated field.

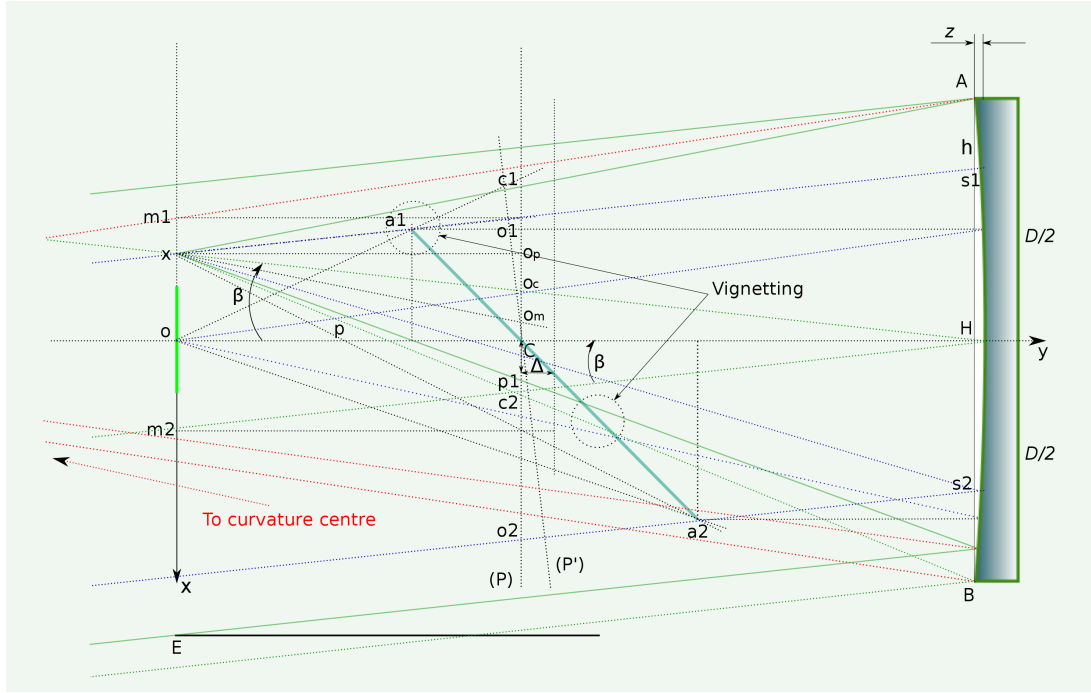


FIGURE 12 – Geometry relative to segment NN' on the focal plane

$$S2 = R_c^2 \left[\pi - \arccos \left(\frac{x_1}{R_c} \right) - \arccos \left(\frac{-x_2}{R_c} \right) + \left(\frac{x_1}{R_c} \right) \sqrt{1 - \left(\frac{x_1}{R_c} \right)^2} + \left(\frac{-x_2}{R_c} \right) \sqrt{1 - \left(\frac{-x_2}{R_c} \right)^2} \right]$$

knowing that :

$$x_2 = O_m(x) - \frac{2O_m(x) - \sqrt{[2O_m(x)]^2 - 4(1-u) \left[\frac{\emptyset_m^2(0)}{4} - R_c^2 + O_m^2(x) \right]}}{2(1-u)}$$

$$S3 = \frac{1}{4} \emptyset_m(0) \emptyset_m(x) \left[\arccos \left(\frac{2(O_m(x) - x_2)}{\emptyset_m(x)} \right) - \frac{2(O_m(x) - x_2)}{\emptyset_m(x)} \sqrt{1 - \left(\frac{2(O_m(x) - x_2)}{\emptyset_m(x)} \right)^2} \right]$$

The formula of the illumination $I_{NN'}(x)$ for this segment NN' is of the same type as that previously shown figure (15). We obtain its representation as a graph by using a calculation program whose result is given figure (14) showing the case of the theoretical telescope here studied as well as a real telescope.

We can now draw an overall view of the illumination curve on the complete diameter of the field of view, parallel to the axis of the telescope, figure (15). Here, the example is

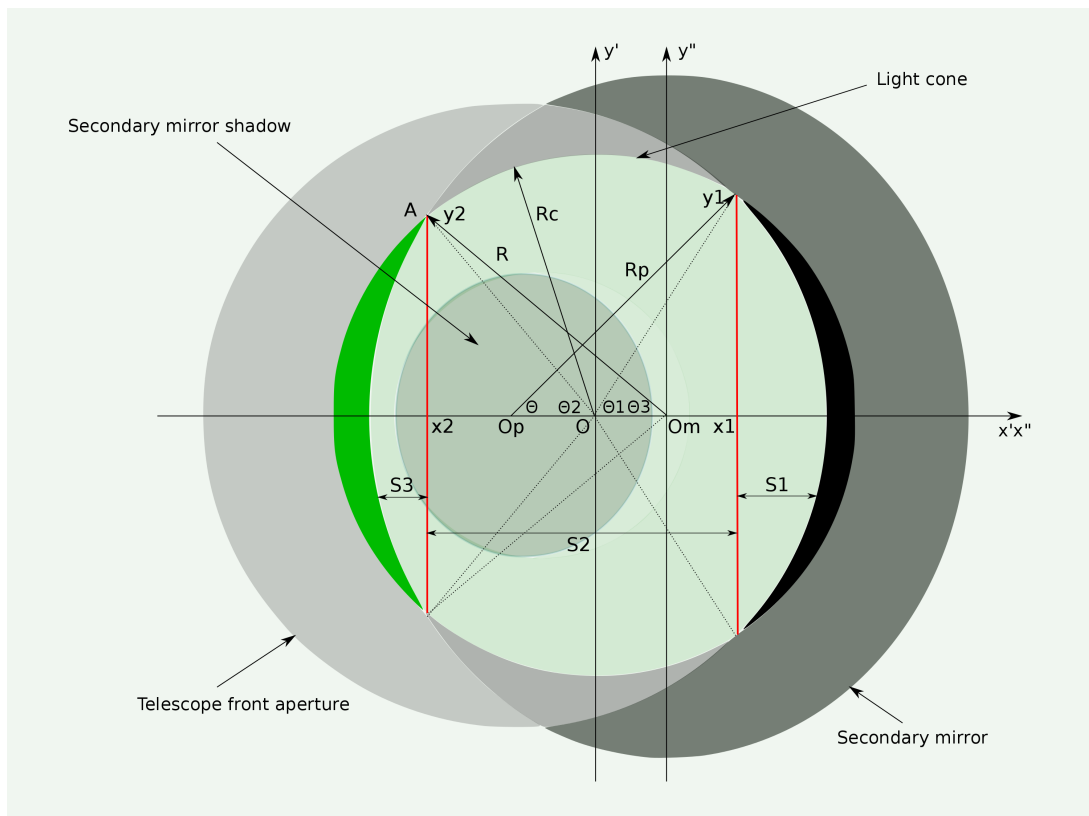


FIGURE 13 – Illumination on segment NN' in plane (P) viewed from point x.

that of a real telescope. We can of course see that the curve is not entirely symmetrical. This is due to the design of the Newtonian telescope and its secondary mirror tilted at 45° whose shape and position produces a dissymmetry.

So we can see that the illumination decreases more rapidly when we move away from the axis of the focal plane on the side opposite to the primary mirror. At the extreme edge of the visual field, the difference reaches about 7%, in the example used here. The coordinates of more or less 25mm starting from the axis correspond to the limits of the focuser half diameter which are used the most and whose diameter is 50,8mm (2 inches).

Figure (15) shows the levels of illumination of the photo sensors (format APS and 24x36). The gaps at one edge and the other are at about 0,5 to 2%. This is difficult, but not impossible to measure. We just need to take 2 photos of the same star, with, let's say, 1 minute of exposure at 800 iso, placing this at the edge of the sensor. Next, using photo-editing software, we just need to compare the ADU³ level of the star in each photo⁴.

3. Analogic Digital Unit

4. If we can't see a difference, the entire previous demonstration needs to be looked at again. . .

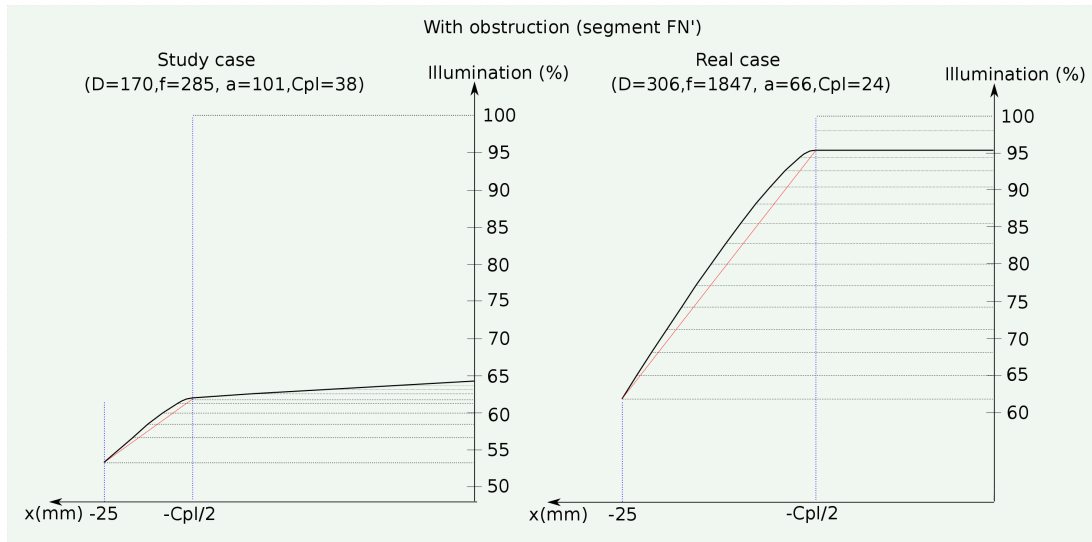


FIGURE 14 – Illumination curve on segment $N'F$ on the focal plane, with obstruction.

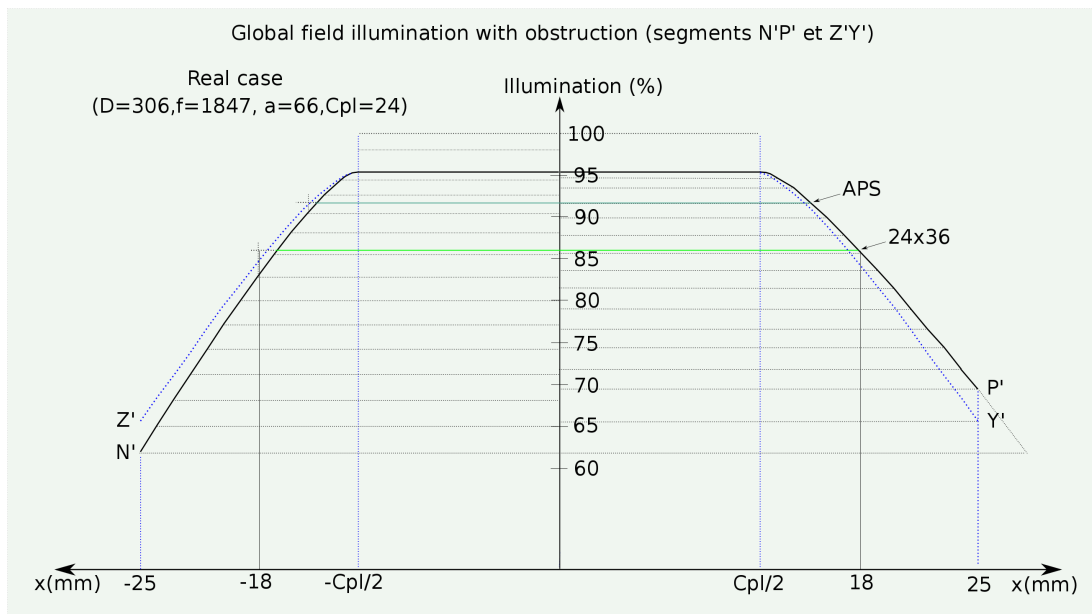


FIGURE 15 – Illumination curves on segments $N'P'$ and $Z'Y'$ on the focal plane, with obstruction.

The illumination on the other diameter of the focal plane is symmetrical in relation to the axis of the latter, in other words $I_{ZZ'}(x) = I_{YY'}(x)$. We can use the initial formula $I_{PP'}(x)$ and just change the parameters of the secondary mirror. Here, the geometry of the problem is a little more subtle (figure 16). The apparent diameter of the secondary

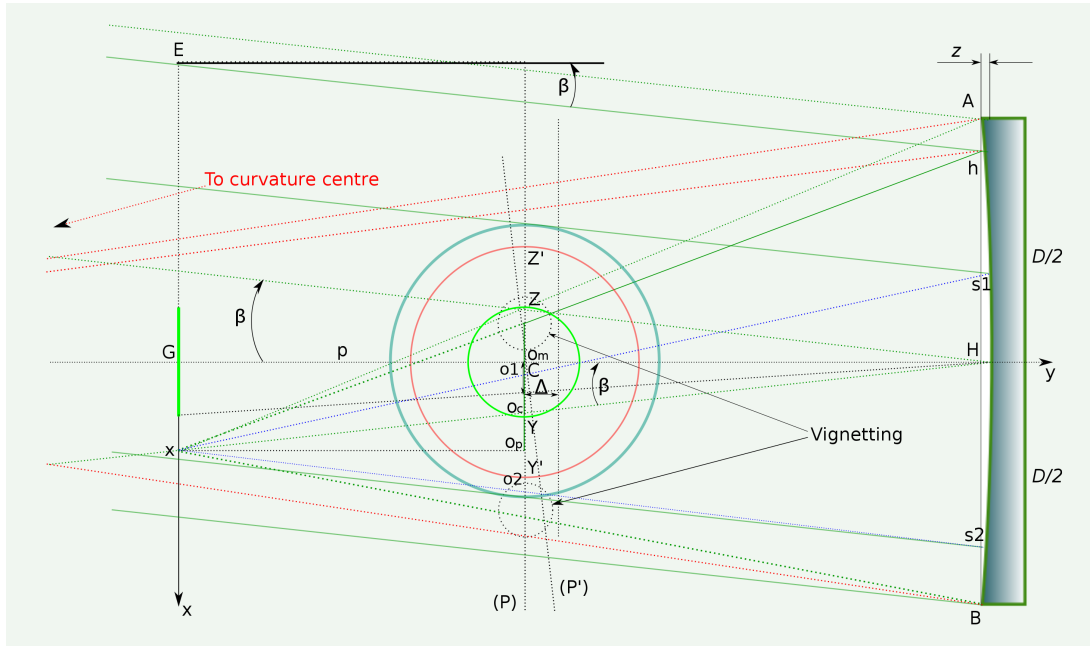


FIGURE 16 – Geometry relative to segment YY' on the focal plane.

mirror viewed from the focus and projected on the plane perpendicular to the primary mirror's axis, and passing through C, is given by the following relation :

$$\varnothing_m(0) = \frac{ap}{p + \Delta}$$

When we move away from the focus, the secondary mirror appears, again, as an ellipse. The ratio of the diameters varies roughly like $\cos\beta$ with $f \tan \beta = x$. We can thus write :

$$\varnothing_m(x) = \frac{ap}{(p + \Delta)\sqrt{\frac{x^2}{f^2} + 1}}$$

We can also see that point Om is mixed with point C, the intersection of the secondary mirror optical centre with the axis of the primary mirror. In the Cartesian coordinate system $x'Oy'$ of plane (P) passing through C previously defined, the coordinate of point Om is given by the following relation :

$$Om = -(f - p)\frac{x}{f}$$

The area of the secondary mirror's shadow is approximately constant here, and equal to $S_{oms}(0)$. By replacing these last 4 parameters in the main formula, we obtain the illumination on segment YY'. The line in figure (15) is shown by the curve marked by a blue dotted line. This is symmetrical in relation to the axis of the focal plane.

Distance to the axis	$I_{PP'}$	$I_{NN'}$	$I_{YY'}$	$I_{ZZ'}$	I_{AVE}	Magnitude lost
12 mm	0,953	0,953	0,953	0,953	0,953	0,05
13 mm	0,947	0,943	0,940	0,940	0,942	0,06
14 mm	0,933	0,926	0,924	0,924	0,926	0,08
15 mm	0,918	0,905	0,906	0,906	0,908	0,10
16 mm	0,900	0,880	0,885	0,885	0,887	0,13
17 mm	0,879	0,855	0,863	0,863	0,865	0,16
18 mm	0,859	0,828	0,841	0,840	0,841	0,19
19 mm	0,837	0,800	0,817	0,817	0,817	0,22
20 mm	0,815	0,771	0,793	0,793	0,793	0,25
21 mm	0,791	0,742	0,768	0,768	0,767	0,28
22 mm	0,767	0,711	0,742	0,742	0,740	0,32
23 mm	0,744	0,681	0,717	0,717	0,714	0,36
24 mm	0,719	0,650	0,692	0,692	0,688	0,40
25 mm	0,694	0,619	0,665	0,665	0,660	0,45

FIGURE 17 – Illumination and loss of magnitude for a real telescope ($D=306$, $f=1847$, $a=66$, $Cpl=24$, $p=272$, $Pu=D+Cpl$)

Figure (15) shows the illumination of 2 diameters $N'P'$ and $Z'Y'$ on the full visual field for a real telescope with optical focal ratio value of 6.

The table in figure (17) gives some values of illumination outside of the fully illuminated field for a real telescope. The loss of magnitude is also indicated relative to the average value of the illumination for a distance given to the axis of the focal plane. The first row of the table gives the values of the illumination on the edge of the fully illuminated field.

3.3 Vignetting caused by the focuser.

On the focal plane, in all telescopes we can find a focuser which is quite elaborate and based generally on the same principle. The cylindrical part of the system, with very varied dimensions of length, produces vignetting in the focal plane. Two elements are important here; on one hand, we have the diameter of the focuser's input aperture and on the other hand, the distance which separates this from the focal plane. In Figure (18), these elements are marked d and l . In most cases, d value is equal to $50.8mm$ (2 inches). The distance l_{max} is the maximum distance beyond which the input aperture will produce vignetting of the fully illuminated field.

In this diagram, in the focal plane, points i , j , k et k' (k' and k are symmetrical in relation to the focus) represent the coordinates below which the focuser's input aperture begins to vignette luminous flux given off by the secondary mirror. These points are found

In practice, it's this last inequality which interests us. The knowledge of l_{max} presumes the knowledge of parameters a , Δ , p and C_{pl} as well as the dimension of the focuser's input aperture. Next, a scaled drawing should indicate how to position this focuser in relation to the tube in the different optic configurations desired at the focal plane.

The vignetting created by the focuser's input aperture superimposes itself onto that studied previously. More precisely, in the focal plane when the distance x in relation to the focus is superior to values i , j ou k , the secondary mirror begins to be vignetted. This means an increase in vignetting and thus a decrease in illumination.

From Figure (18) we can easily calculate the diameter and position of the focuser's input aperture in plane (P) :

$$\text{Ø}_{p_{smap}} = \frac{dp}{l} \text{ and } x' = \frac{2x(l-p) + dp}{2l}$$

In this figure we also have a circle (marked with a dotted line) representing the projection of the secondary mirror in plane (P) viewed from the focus. This is a way to see what happens to diameter $Z'Y'$ on the focal plane. Its diameter in plane (P) is thus $\frac{pa}{p+\Delta}$.

We can now deduce the position of centre Op_{smap} in the Cartesian coordinate system $x'Oy'$ of plane (P), bearing in mind that the origin of this system corresponds to that of the projection of the light cone on the same plane :

$$Oc = c2(x) - R_c = x \left[1 - \frac{p}{(f-z)} \right]$$

$$Op_{smap} = x' - \frac{\text{Ø}_{p_{smap}}}{2} - Oc = x \left[\frac{l-p}{l} - 1 + \frac{p}{(f-z)} \right]$$

The intensity of the vignetting depends on the variable l , the distance of the input aperture from the focal plane. In figure (19) which represents the elements of the telescope in plane (P) viewed from point x , this supplementary vignetting has been added.

We can now calculate the area of the primary mirror which illuminates point x on the focal plane, keeping in mind the vignetting caused by the focuser. On segment PP' , the function $I_{PP'}(x)$ previously studied remains valid as long as $x \leq i$. When $x > i$ we must simply modify the calculation of $S3$ and of $x2$. In this case, $S3$ is the segment of a circle whose area is given by the following expression, knowing that $R_s = \frac{dp}{2l}$:

$$S = \frac{r^2}{2} [2\theta + \sin(2\theta)] \text{ where here } R_s \cos \theta = x_2 - Op_{smap} \text{ then } \theta = \arccos \frac{x_2 - Op_{smap}}{R_s}$$

Knowing that $\sin(2 \arccos(x)) = 2x\sqrt{1-x^2}$ we obtain for this area :

$$S3 = R_s^2 \left[\arccos \left(\frac{x_2 - Op_{smap}}{R_s} \right) - \left(\frac{x_2 - Op_{smap}}{R_s} \right) \sqrt{1 - \left(\frac{x_2 - Op_{smap}}{R_s} \right)^2} \right]$$

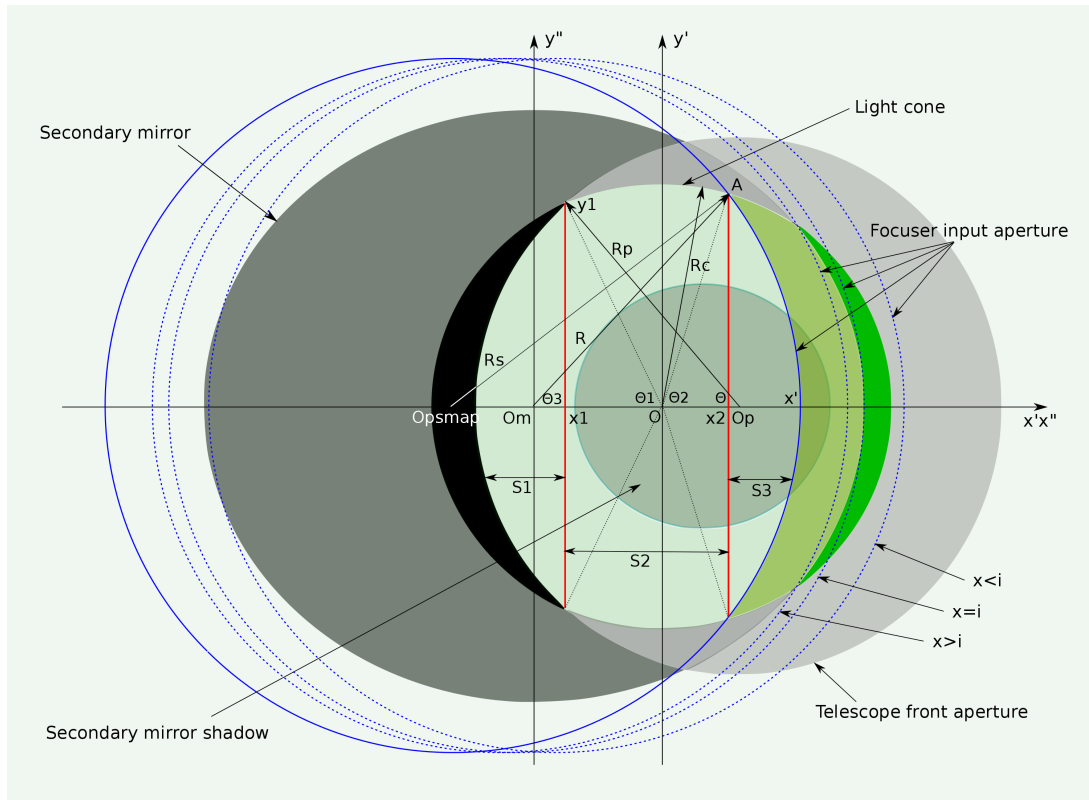


FIGURE 19 – Vignetting on segment PP' caused by the focuser's input aperture.

In figure (19), x_2 is the coordinate of point A which is both on the circle of radius R_s and on that of radius R_c . To determine x_2 , we just need to solve the following system :

$$\begin{aligned} R_c^2 &= y_2^2 + x_2^2 \\ R_s^2 &= y_2^2 + (x_2 - Op_{smap})^2 \end{aligned}$$

And so :

$$x_2 = \frac{R_c^2 - R_s^2 + Op_{smap}^2}{2Op_{smap}}$$

We now need to replace these two parameters in the formula $I_{PP'}(x)$ in order to take into account the vignetting caused by the focuser's input aperture, and when at the focal plane $x > i$.

Strictly speaking, the preceding formula is only applicable if the value of x_2 is inferior or equal to that obtained in section (3.2.4). Indeed, there is a small space close to i whose area is more difficult to calculate. This is due to the fact that the vignetting caused by the focuser's input aperture is not yet preponderant. We can take this into account *javascript*

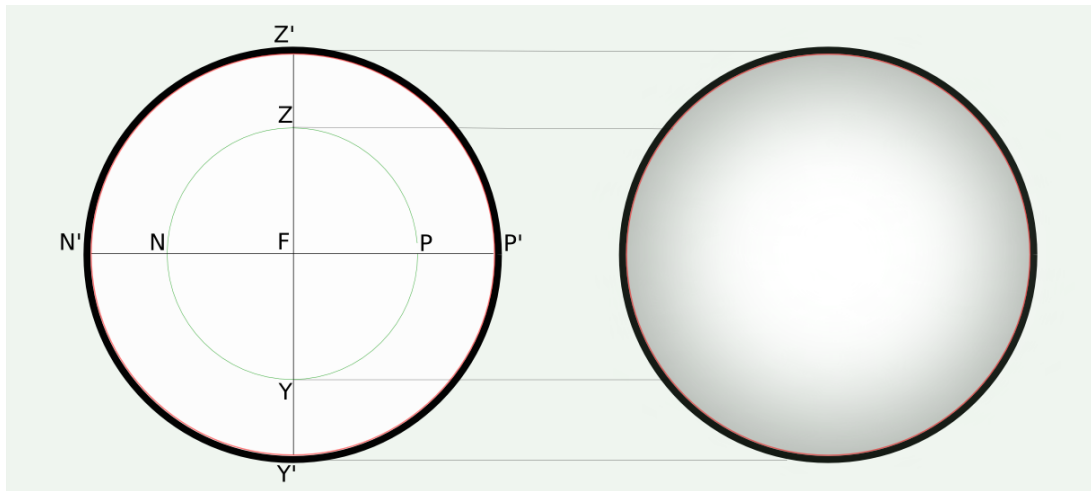


FIGURE 20 – Imagery of the illumination of the full visual field on the focal plane.

or php and proceed by extrapolation, but we are here dealing with a space of only about a millimeter!

For segments ZZ' and YY' the formula to use is the same as the previous one, with respectively $x > k$ and $x > k'$. And, finally, still with the same formula but with x being negative, we obtain the illumination of segment NN' .

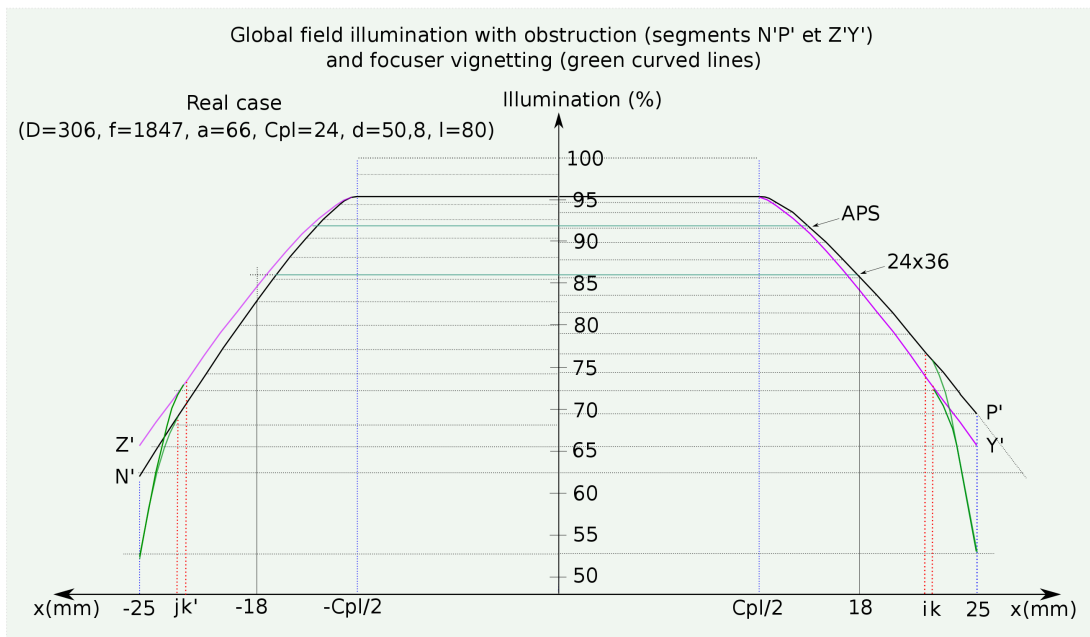


FIGURE 21 – Addition of vignetting caused by the focuser's input aperture.

Distance to the axis	$I_{PP'}$	$I_{NN'}$	$I_{YY'}$	$I_{ZZ'}$	I_{AVE}	Magnitude lost
23 mm	0,713	0,681	0,713	0,713	0,713	0,36
24 mm	0,623	0,622	0,622	0,622	0,622	0,51
25 mm	0,528	0,527	0,528	0,528	0,528	0,69

FIGURE 22 – Illumination at the edge of the field of view with vignetting caused by the focuser for a real telescope ($D=306$, $f=1847$, $a=66$, $C_{pl}=24$, $p=272$, $Pu=D+C_{pl}$, $d=50.8$, $l=80$)

Figure 21 shows the illumination curve while taking into account the vignetting caused by the focuser (green curve). We can clearly see, at the edge of the field of view, a significant drop in illumination which in this example reaches almost 50%. And finally the table figure 22 indicated the corresponding values as well as the loss of magnitude which results from this.

4 Front aperture of the telescope.

Pu is the diameter of the telescope's front aperture, at a distance f from the primary mirror and presuming here that the parameters D , a , f , C_{pl} , d and l are now fixed. In the previous section, we took a look at the illumination of the fully illuminated field on the focal plane, with a telescope front aperture of diameter $D + C_{pl}$ and positioned at a distance f from the primary mirror. This diameter corresponds to a minimum for a given fully illuminated field. To slightly increase the illumination beyond the fully illuminated field, we can calculate this as the diameter of the front aperture which no longer vignettes the light cone at the edge of the field. By taking the preceding parameters, we can see that we only need R_p to be equal to $Op + R_c$ in plane (P) or that x_1 be equal to $-R_c$ with $S1(x)$ which cancels itself out. We can thus deduce the following identity :

$$R_p = Op + R_c \text{ soit } R_p = \frac{px}{(f-z)} + \frac{pD}{2(f-z)} \text{ where finally } R_p = \frac{p(D+2x)}{2(f-z)}$$

This result is to be compared with $R_p = \frac{p(D+C_{pl})}{2(f-z)}$ in the previous section for $Pu = D + C_{pl}$. Here, on the edge of the field, x is equal to $\frac{d}{2}$, and we can thus deduce that the actual diameter of the telescope's front aperture, always at a distance f from the primary mirror, should simply be :

$$Pu_{max} = D + d$$

With d being the diameter of the focuser, and D being the diameter of the primary mirror, this value can be considered as a maximum, beyond which we cannot obtain

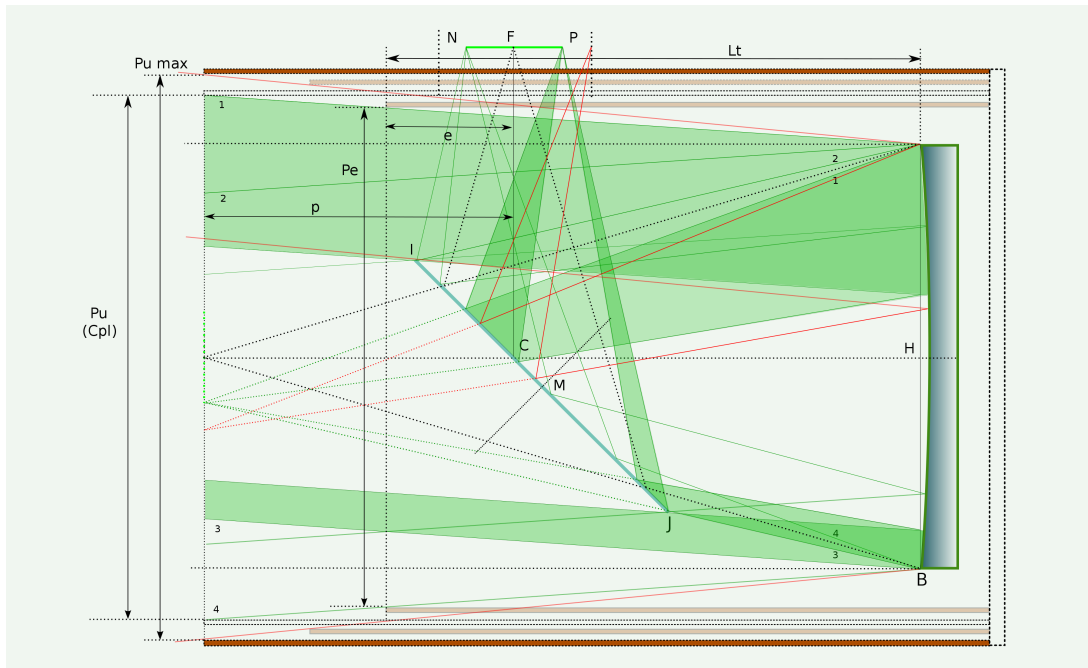


FIGURE 23 – The dimensions of the telescope’s front aperture and of the tube.

any more illumination on the focal plane. The formulae giving the illumination become simplified, as $S1(x) = 0$, and $S2(x)$ is reduced to x_2 terms. In this case, we obtain the values given in the tables⁵ figure 24 and 25, without and with vignetting caused by the focuser. We can see that the illumination on the edge of the field has increased by several percent (4%), in relation to the values found when Pu was equal to $D + C_{pl}$. Visually, this would not be of particular significance, but in any case a little more light is always a good thing!

From a more practical point of view, at a distance f from the primary mirror, the diameter of the telescope’s front aperture, Pu , must verify the following expression :

$$D + C_{pl} \leq Pu \leq D + d$$

With the parameters of the real telescope having been seen previously, Pu must thus have a value between 330 and 356 millimetres for a mirror with a diameter of 306 millimetres.

Still from a practical point of view, and in order to reduce the bulk and weight of the telescope a little, we can reduce the diameter of the telescope’s front aperture while still keeping the same illumination on the focal plane. In figure 23, Pe is noted as the diameter of the telescope’s front aperture, but this time at a distance e from the axis of the focal

5. In these two tables, the average values are close to those of several formulae on the Net.

Distance to the axis	$I_{PP'}$	$I_{NN'}$	$I_{YY'}$	$I_{ZZ'}$	I_{AVE}	Magnitude lost
12 mm	0,953	0,953	0,953	0,953	0,953	0,05
13 mm	0,947	0,944	0,941	0,941	0,945	0,06
14 mm	0,936	0,929	0,927	0,927	0,931	0,08
15 mm	0,922	0,910	0,910	0,910	0,915	0,10
16 mm	0,907	0,889	0,893	0,893	0,897	0,12
17 mm	0,890	0,866	0,873	0,873	0,876	0,14
18 mm	0,872	0,842	0,854	0,854	0,856	0,17
19 mm	0,854	0,818	0,834	0,834	0,834	0,20
20 mm	0,835	0,792	0,813	0,813	0,812	0,22
21 mm	0,815	0,766	0,792	0,792	0,789	0,25
22 mm	0,795	0,739	0,770	0,770	0,766	0,29
23 mm	0,775	0,713	0,749	0,749	0,743	0,32
24 mm	0,754	0,686	0,727	0,727	0,719	0,35
25 mm	0,733	0,658	0,704	0,704	0,695	0,39

FIGURE 24 – Illumination on the edge of the field with $Pu=D+d$ and for a real telescope ($D=306$, $f=1847$, $a=66$, $Cpl=24$ and $p=272$)

Distance to the axis	$I_{PP'}$	$I_{NN'}$	$I_{YY'}$	$I_{ZZ'}$	I_{AVE}	Magnitude lost
23 mm	0,745	0,713	0,658	0,658	0,694	0,40
24 mm	0,659	0,657	0,658	0,658	0,658	0,45
25 mm	0,568	0,567	0,567	0,567	0,567	0,61

FIGURE 25 – Illumination with vignetting caused by the focuser, with $d=50.8$, $l=80$ and the parameters seen in figure 24.

plane. We can thus deduce the following relations :

$$\frac{P_u - D}{f - z} = \frac{P_u - P_e}{p - e} \text{ thus : } P_e = P_u \left[1 - \frac{(p - e)}{(f - z)} \right] + D \frac{(p - e)}{(f - z)}$$

when $P_u = D + d$:

$$P_e = D + d \left[1 - \frac{(p - e)}{(f - z)} \right] \text{ and we also have : } L_t = f - z - p + e$$

And so, we must find the right value for the variable e . This will depend on the size of the focuser as well as the regulating mechanism of the secondary mirror. In this case, a scale drawing will again provide a solution for each. In the case of a DOBSON, this value can be only a few centimetres, but in general we can fix the value of e at $\frac{2p}{3}$ or $\frac{p}{2}$. Concerning the total length of the tube, this will depend of course on the thickness of the primary mirror and its holder, which here can again be very diverse. In any case, once the value of e is known, the formulae giving P_e and L_t remain applicable.

5 Field curvature and coma.

In instrumental astronomy, telescopes are affected by a field curvature. Focal points are not all found on a single plane, perpendicular to the optical axis. This is also, of course, true for the parabolic mirrors in Newtonian telescopes. The field curvature (called the PETZVAL surface) is here equitable to a parabolic surface, as the below formula indicates, giving the difference in focus at a distance d from the optical axis on the focal plane :

$$e = \frac{d^2}{2f}$$

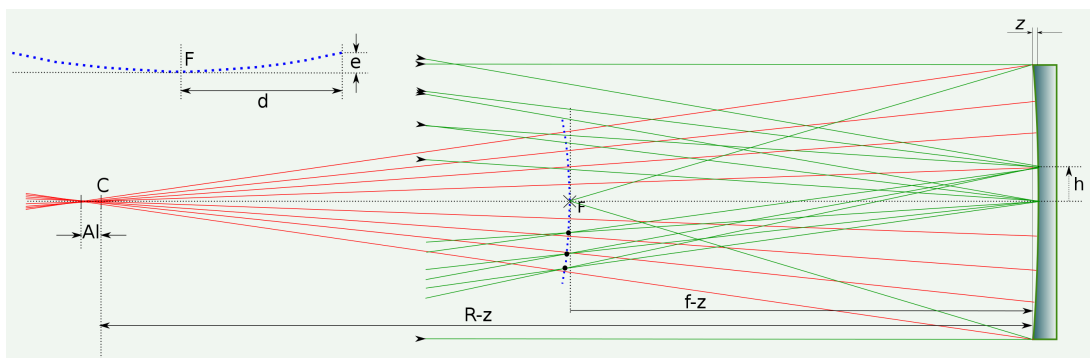


FIGURE 26 – Field curvature.

distance to the axis (d) mm	3	5	8	10	12	15	20
defocus (e) unit μ with $f = 800\text{mm}$	5	15	40	62	90	140	250
defocus (e) unit μ with $f = 1000\text{mm}$	4	12	32	50	72	100	200
defocus (e) unit μ with $f = 1200\text{mm}$	3	10	26	41	60	93	166
defocus (e) unit μ with $f = 1500\text{mm}$	3	8	21	33	48	75	133

FIGURE 27 – Field curvature, deviation on the focal plane.

The numerical values in the table seen in figure 27 are to be compared with what we call the depth of focus, or focusing tolerance, which is acceptable. This is a space on the focal plane, in which we can place a sensor in order to have a sharp image. In various writings on the subject we can find the following formula for this space :

$$T_{map} = \pm 8\Delta n\lambda \left(\frac{f}{D}\right)^2 \quad (16)$$

Here, Δn represents a difference between the wave fronts with a value of $\frac{1}{4}$ and λ is the average wavelength, which is 550 nm (visible). The table in figure 28 gives several values for the focusing tolerance in microns on the focal plane corresponding to the relation f/D .

f/D	3	4	5	6	10	15	20
$T_{map}(\mu)$	± 10	± 18	± 22	± 40	± 110	± 248	± 440

FIGURE 28 – Focusing tolerance in microns.

Visually, the field curvature in a Newtonian telescope has very little effect, as the human eye is easily able to adapt. In astrophotography, this field curvature can lead to a loss of sharpness, in the case of a small instrument with a high focal ratio and a large sensor. For example, a 200mm Newtonian telescope with a focal ratio of 4, has a focusing tolerance of 35 microns and a defocus of about 60 microns at 10mm from the axis. In this case, a photo taken with an APS sensor could be sharp in the middle, but not around the edges. This case is a little particular, as in general Newtonian telescopes with a focal ratio of 4 or less have substantial diameters as well as large focal lengths. We can generally consider that the field curvature in Newtonian telescopes is acceptable. In planetary photography, with the relations f/D in excess of 10, we can altogether ignore this field curvature.

The most critical aberration for Newtonian telescopes is the coma. This appears rather quickly on the focal plane, as soon as we move away from the optical axis. The oblique rays stretch the images of stars, thus making them appear more like comets! The geometry of this coma aberration is indicated in figure 29. It is established that the incident rays at a

height h_i on the primary mirror form a circle on the focal plane, whose diameter is given by the following relation :

$$M_i = \frac{dh_i^2}{2f^2} \text{ as well as } M_i = K_i$$

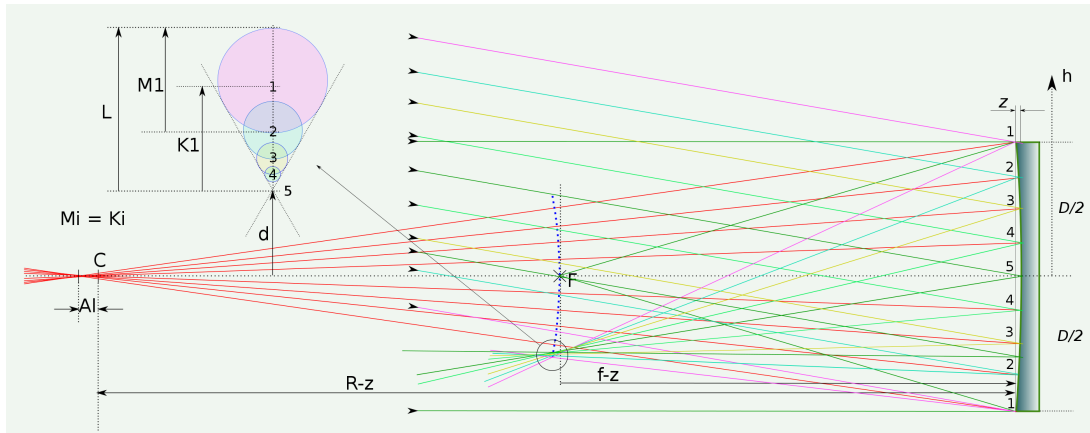


FIGURE 29 – Coma.

The total length of this diagram of a coma at a distance d from the axis is thus $M_1 + \frac{M_1}{2}$ with $h_1 = \frac{D}{2}$ and so :

$$L_{coma} = \frac{3d}{16 \left(\frac{f}{D}\right)^2} \tag{17}$$

distance to the axis (d) mm	3	5	8	10	12	15	20
length coma (μ) with $f/D = 3$	62	104	166	208	250	312	416
length coma (μ) with $f/D = 4$	35	58	93	117	140	175	234
length coma (μ) with $f/D = 5$	22	37	60	75	90	112	150
length coma (μ) with $f/D = 6$	15	26	41	52	62	78	104

FIGURE 30 – Coma length in microns.

The numerical values in the table shown in figure 30 clearly demonstrate that the coma effect appears very quickly, even when close to the axis (for example, with a mirror of focal ratio 4 and at 10mm from the axis, the length of the coma would be at about 100μ). And so, with an APS sensor and 5μ pixels, the coma at the edge of the image would cover 20 pixels ! In astrophotography, for deep sky imaging, the use of a coma corrector is

essential. The best-known models are ROSS and WYNNE. These correctors are specifically calculated for a given focal length and a primary mirror diameter.

This matching between the parabolic mirror and its corrector must be studied with great care by constructors, as the quality of the photo depends on it. We can see here that the higher the focal ratio of the parabolic mirror, the more significant the coma becomes and so the more precise the corrector must become⁶.

Figure 29 outlines how the incident rays converge after reflection in the parabolic mirror. Here, the normals used for drawing the lines are the rays of the parabola curves. These converge towards a segment called the longitudinal aberration. The centre of curvature C corresponds to the radius of the curvature of the centre of the mirror, marked R in the diagram. At a distance h from the centre of the mirror, the corresponding longitudinal aberration is worth approximately :

$$A_{long} = \frac{h^2}{R(0)} \text{ with } R(0) = 2f$$

6 Collimation.

We cannot finish a document about Newtonian telescopes without talking about collimation, which we can already find described in hundreds of books and web pages on the subject! Nevertheless, here's yet another description, to end our document. After a few general comments on this subject, and on the equipment to use, the collimation will be described in six steps. The first five are basic essentials which follow on from the design itself of a Newtonian telescope, and must be carried out with care. This is the geometric collimation. If we wish to have a more detailed adjustment for astrophotography, it will be necessary to work uniquely with the placement of the primary mirror (when observing a real star to high magnification). The objective here is to get as close to a perfect collimation as possible.

The essential steps for aligning and collimating the two mirrors are :

- Adjustment of the focuser's axis, secant and orthogonal to the tube's axis.
- Positioning of the primary mirror on the tube's axis.
- Positioning of the secondary mirror on the axis of the focuser.
- Orientation of the secondary mirror.
- Orientation of the primary mirror.
- Precise collimation on a real star.

6. C'est donc la double peine au niveau du porte-monnaie

6.1 A few initial remarks.

- As has also been said a hundred times before, a bad collimation has an extremely negative impact on the performance of an instrument, even one with a high-quality optical system. This is applicable to all telescopes, particularly for Newtonian telescopes which because of their design need regular verification of the alignment of their mirrors. In other words, each time the instrument is transported and set up, some time must be spent on these types of checks. This may even be necessary several times during one viewing session, when the telescope must be moved for example from viewing the East to the West. The meridian transit on a German Equatorial Mount can often be critical for collimation.
- The alignment of the two mirrors can seem relatively simple to deal with. Indeed, we just need to ensure that when viewed from the focuser, the different elements are laid out concentrically. However, experience shows that this operation is not as simple as it may seem. Additionally, the way in which each of us interprets what we see is not necessarily the same.
- The precision obtained is completely relative, since adjustments are initially carried out using only the naked eye, and involve macroscopic elements. Refining the image of a star is essential when using a telescope for astrophotography. The adjustments are in this case carried out on a highly magnified image. We can thus obtain a precision of a few microns, as we are here on a level with the Airy disk.

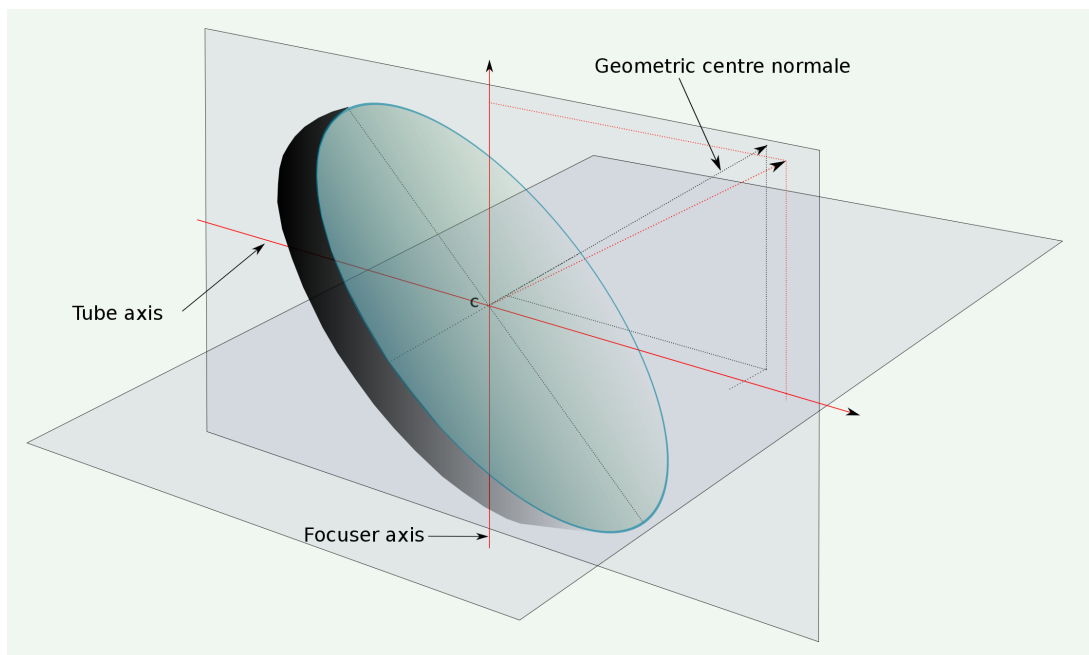


FIGURE 31 – Secondary mirror : correct position but no orientation.

- Amateur astronomers who use commercial telescopes can feel a certain apprehension when dealing with the complete removal of the two mirrors, and when thinking about putting them back again in the correct way afterwards. This is just a psychological barrier which must be overcome. Here, the total collimation begins to make sense and will provide a real satisfaction to the user, as well as a better knowledge of their telescope, once of course everything has been set up again correctly.
- In the following sections, we will make the difference between the positioning and the orientation of the mirrors, even if these two things sound very similar. The positioning here refers to that of the centre of the mirrors on the axes (the geometric centre of the primary mirror and the optical centre of the secondary mirror). The orientation of the mirrors concerns the direction of the normal, relative to the points of intersection with the axes. When the centre of the mirror is well positioned, there is an infinity of possible orientations of the normal to this centre, and thus to the complete mirror. This is where the interest lies in making the distinction previously mentioned, in order to concentrate on one action at a time during each step. In figure 31, for example, the secondary mirror is well positioned, with the optical centre C on the intersection of the two axes, but it is not correctly oriented, with the normal at point C not being on the plane of the two axes and at 45 degrees.

6.2 The equipment to be used.

The basic tool to carry out collimation is called the 'collimating eyepiece', or collimator. On each of its ends are found, respectively, a peephole and a crosshair (figure 32). Its main function is to check the alignment mirrors centered with the axis of the focuser. The ideal thing would be to make this sighting tool oneself, and this doesn't present any particular problem. Otherwise, we can find a range of products in shops today, the best-known being the 'Cheshire' type, which is a little more evolved than simple collimators. They comprise an aperture and a reflective surface inclined at a 45 degree angle, allowing a better view of the crosshair.

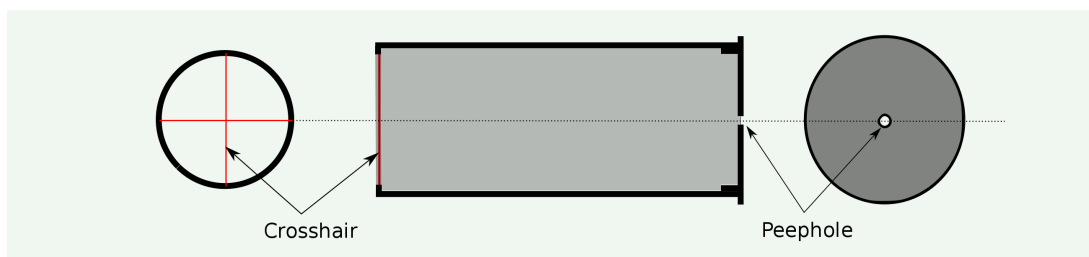


FIGURE 32 – A simple collimator

As Figure 33 shows, these sighting tools must combine two contradictory imperatives. The crosshair must be far enough from the eye to be sharp, and the length of the collimator

must enable a complete view of the secondary mirror. In practice, it is difficult to focus on the crosshair, except for those with a very flexible eye lens. . .

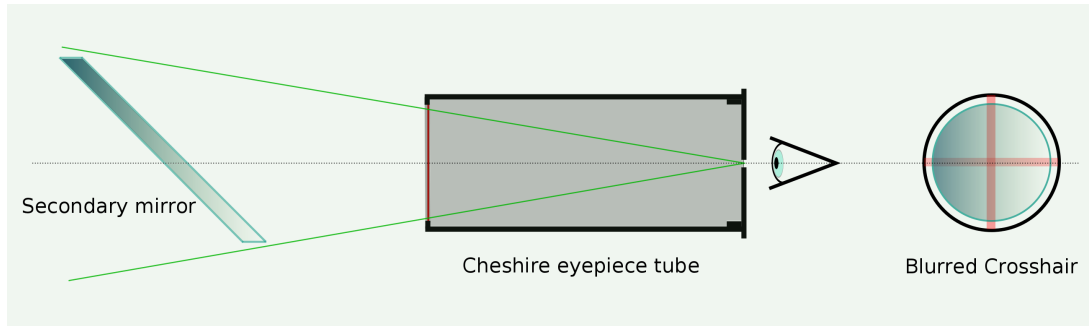


FIGURE 33 – Collimator problem.

Another tool proves very useful for rapidly orienting the two mirrors, when they are both well positioned. This is a laser collimator which is placed in the focuser. The laser beam goes back and forth from the primary mirror, passing by the secondary mirror. The mirrors are correctly oriented when the two beams merge together. The return beam can be visible on frosted glass.

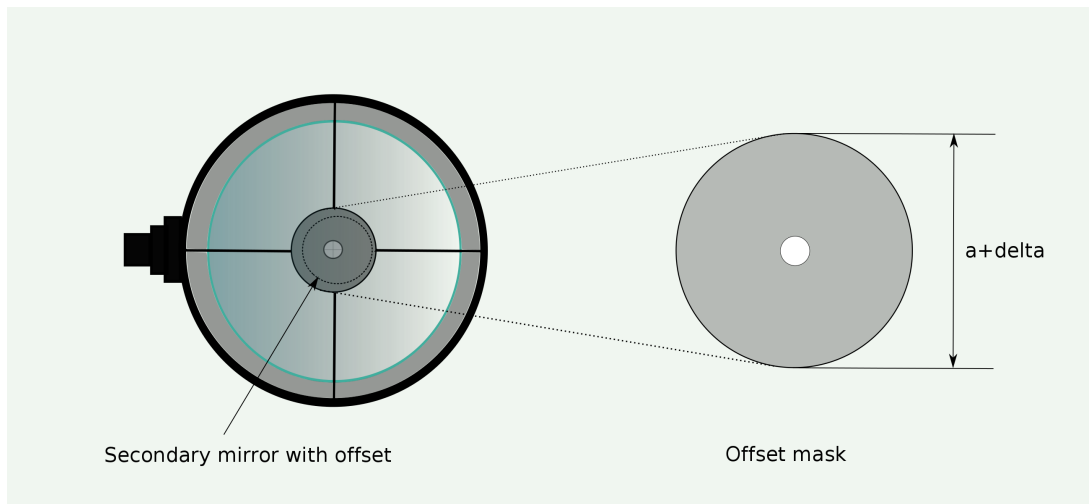


FIGURE 34 – Delta mask.

The discrepancy Δ (offset) of the secondary mirror in relation to the axis of the primary mirror and so the tube axis can be a source of errors when making adjustments. We can effectively perceive that the secondary mirror is slightly off-centre when we observe its reflection in the primary mirror. In order to avoid this effect, we can make a delta-mask, which is fixed centrally onto the secondary mirror's holder, at the entrance of the tube.

This must have a diameter at least equal to the secondary mirror's minor axis, to which the discrepancy Δ must be added (see figure 34).

For the final phase of collimation, let's practice on an artificial star. This can be simulated using a very bright spotlight, with a diameter of few microns. It can be used even in the middle of the day, and does not require a sidereal follow-up. Unfortunately, this light source, which is situated 15 or 20 metres away, forms image far from the focal plane and requires a special setup. This artificial star can be useful for a Schmidt-Cassegrain telescope, but is not well adapted to a Newtonian telescope.

It's also worth noting that the cost of such a case (for the spotlight), or of a laser collimator, is completely insignificant in relation to the cost of the complete configuration for astrophotography. We would thus be wrong to deny ourselves these extras!

There are also other tools which can be quite useful for collimation; this is a vast subject and from time to time, new ones appear. Everyone can find what they need on the internet.

6.3 Adjustment of the focuser's axis, secant and orthogonal to the tube's axis.

This involves a basic adjustment, to be carried out as soon as we attach a focuser to the tube. With commercial telescopes, this adjustment has usually been made in the factory. However, we cannot be certain that it is completely correct, and so in order to erase any doubt, we can carry out this adjustment at least once ourselves.

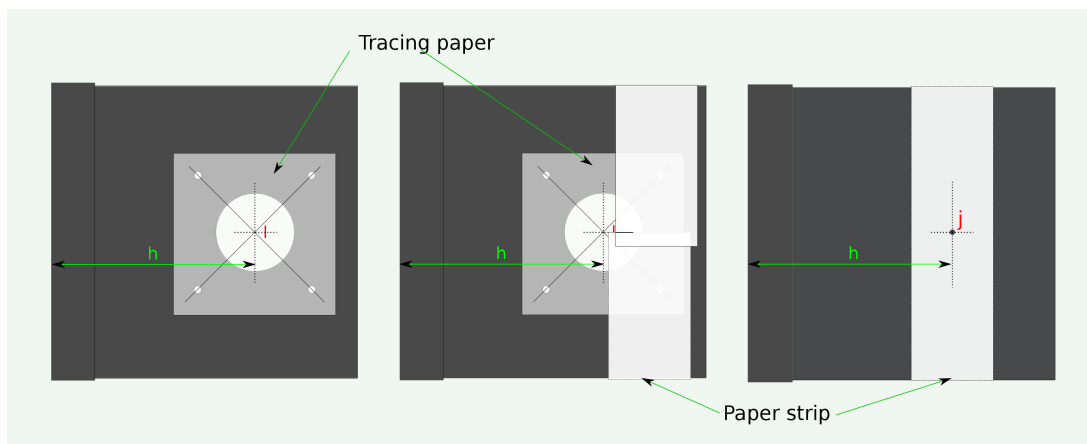


FIGURE 35 – Materialisation of the focuser's axis on the tube.

In order to do this, we must first remove the secondary mirror as well as the focuser which is fixed to the tube with four screws. As figure 35 shows, with the help of tracing paper we can draw the diagonal lines passing through the holes from the four screws.

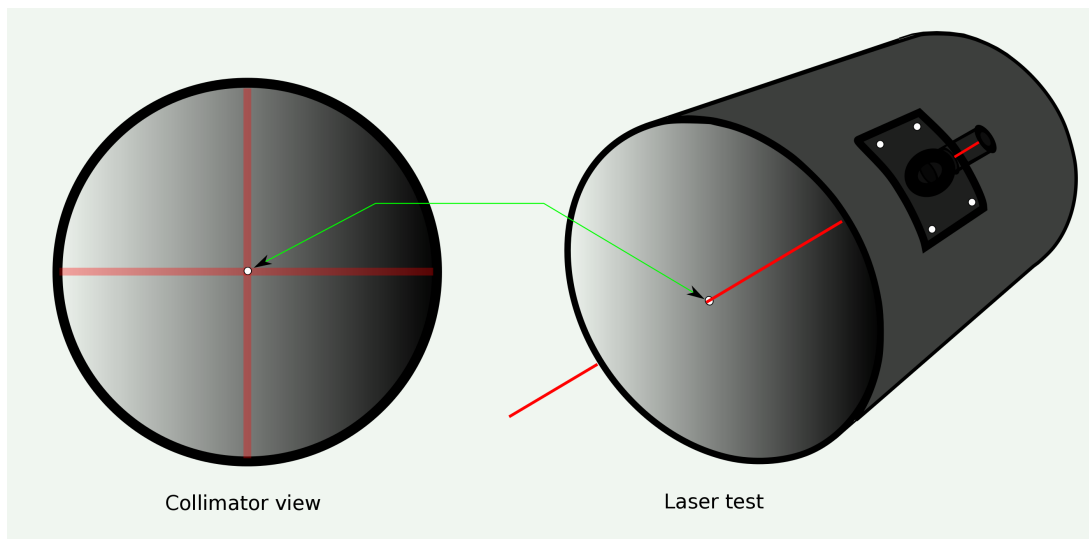


FIGURE 36 – Verification of the focuser's axis.

These normally intersect on the focuser's axis at point I . It is thus necessary to find point J , symmetrical to I in relation to the tube's axis and, materialise this point in the interior of the tube.

There are several methods for this, but we can simply use a strip of paper to measure very exactly the external perimeter of the tube, and deduce from this the position of point J (half perimeter). We then need to pierce the tube at this point, using a 1mm bit, for example.

We can thus replace the focuser, checking with the laser or the collimator that the small hole visible on the opposite side of the tube is well aligned. If this is not the case, we must adjust the four screws, using precise washers. The laser collimator beam must go through the tube passing exactly through the small hole.

6.4 Positioning of the primary mirror on the tube's axis.

This adjustment is also, of course, implicit. The primary mirror's axis must merge with the tube's axis. With commercial telescopes, the centring of the primary mirror in its holder is normally correct, and carried out in the factory. It is nevertheless necessary to check this adjustment each time that the primary mirror is removed for cleaning.

Although the primary mirror shouldn't undergo any stress, we can potentially use small cork wedges to avoid it from being moved off-centre. A simple ruler should enable the mirror to be centred to a within a quarter of a millimetre, even a tenth of a millimetre for those with good eyesight. As indicated in figure 37, we can base our case on the measurement from the edge of the mirror to the interior edge of its holder, and on three or four different places.

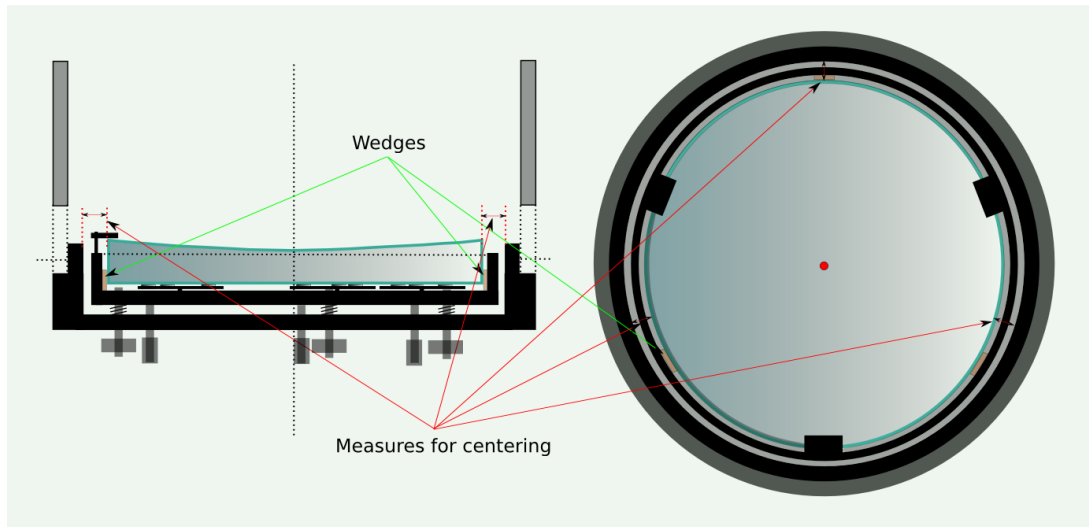


FIGURE 37 – Centring of the primary mirror.

6.5 Positioning of the secondary mirror.

Here we will look at the first thing to deal with concerning the secondary mirror. The positioning of this mirror consists in placing the optical centre C at the intersection of the focal plane axis, and that of the primary mirror.

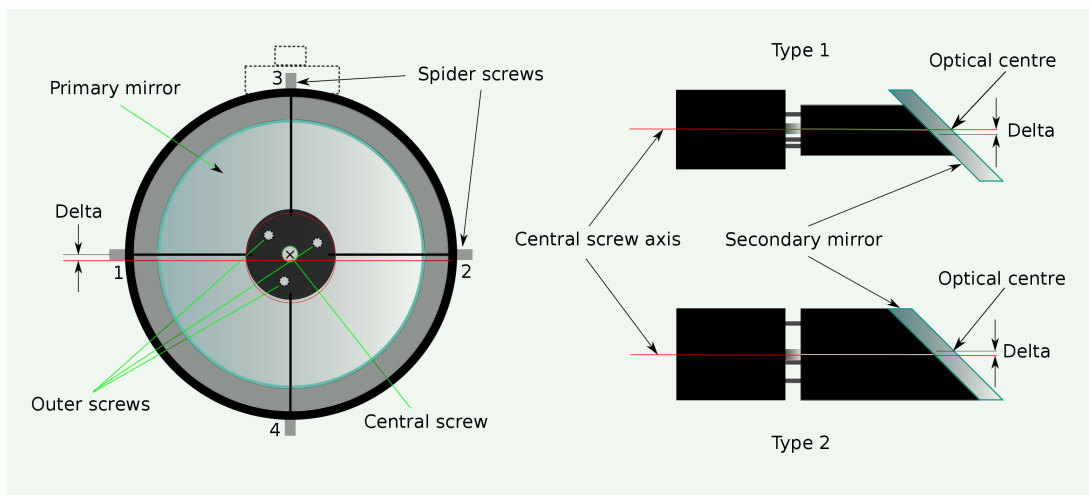


FIGURE 38 – Positioning of the spider.

Before doing this, we need to check the position of the secondary mirror's holder and spider, at least once in order to be confident. As indicated in figure 38, there are essentially two possible cases depending on the type of stand used for the secondary mirror. Generally,

in commercial telescopes the secondary mirror is glued onto its stand, taking into account the offset (type 1). In this way, the optical centre C is on the axis and in this case the spider must be centred. With a simple ruler, and by moving screws 1 and 2, then 3 and 4, the adjustment is simple.

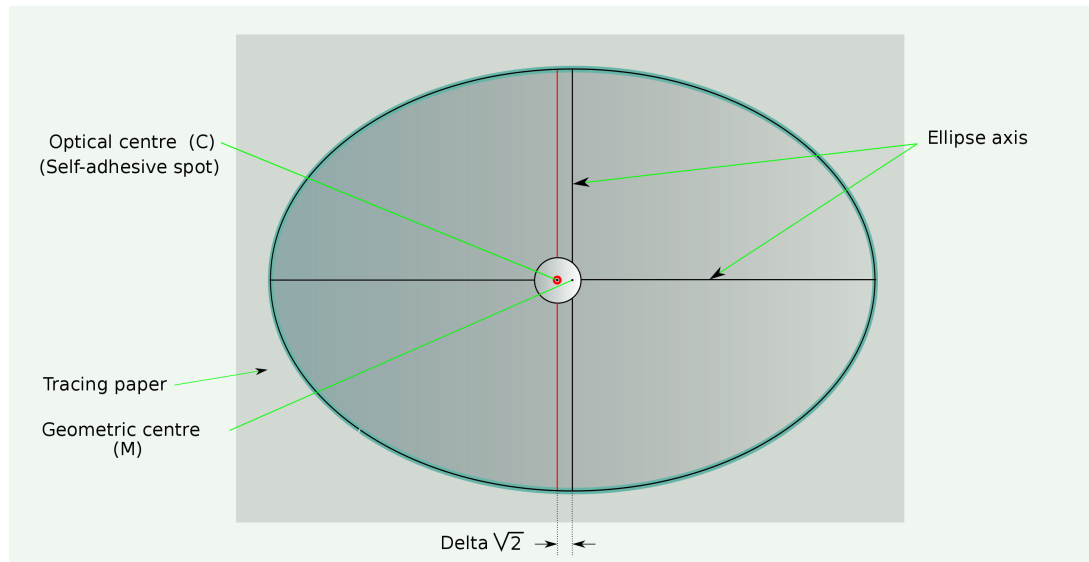


FIGURE 39 – Marking optical centre C on the secondary mirror.

The other case (type 2) is a more classic one among amateur constructors. Here, the optical centre C is not situated on the axis. In order to take into account the offset, we can use screws 3 and 4, and in this way lower the spider to the correct position.

We are now sure that the optical centre C will be very close to the tube's axis, and thus that of the primary mirror.

Before remounting the secondary mirror and its stand on the spider, it could be useful to mark the optical centre C on the secondary mirror. With the help of tracing paper and a precise sketch, we can then create a small opening in order to access the surface of the mirror and to attach a small sticker to it (see figure 39). The most difficult thing here is to find a small enough sticker, but a felt-tip pen will do just as well.

In order to avoid being bothered by the reflection from the primary mirror, we are going to use two cardboard masks in two different colours (in this case, green and purple). One will be placed across the tube and perpendicular to its axis, between the mirrors and quite close to the secondary mirror. The other will be placed on the inside of the tube, opposite the focuser. This will enable us to concentrate only on the secondary mirror.

By using the collimator fixed on the focuser, through the peephole we can see the secondary mirror as shown in figure 40. The three collimation screws have been loosened, and by adjusting the central screw we can centre the secondary mirror. Here we must concentrate on the edge of the secondary mirror as well as the front aperture of the

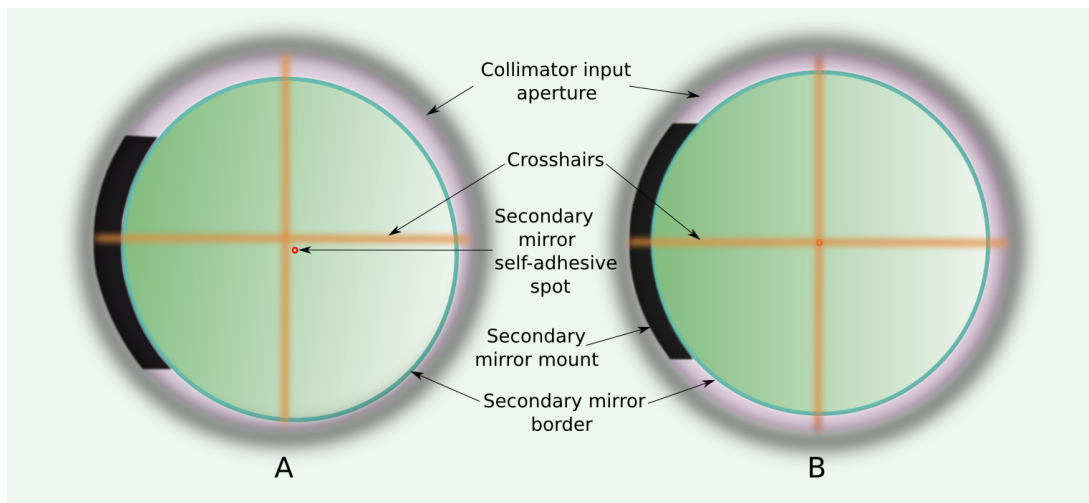


FIGURE 40 – Positioning of the secondary mirror.

collimator, which must both be concentric. For this, we must manually move the mirror so that it appears as a circle. We must obtain what is shown in figure 40 diagram B.

From this point onwards, we must no longer touch the central screw. The only role here of the three collimation screws is to keep the secondary mirror balanced. This initial adjustment is sometimes difficult to do the first time, but everyone can eventually and easily find the best method that suits them in order to obtain the required best result.

6.6 Orientation of the secondary mirror.

This is the most difficult step to carry out. We must now remove the coloured mask which was previously placed across the tube. Through the collimator's peephole, we can now see the reflection of the primary mirror as well as the other elements of the telescope (see figure 41 A).

Things here may seem complicated but we simply need to concentrate on three elements : the collimator's front aperture, the edge of the secondary mirror and the edge of the primary mirror. We can ignore the image of the spider and the focuser reflected in the secondary mirror, then the primary mirror and again in the secondary mirror.

By moving the three collimation screws of the secondary mirror, we must then gradually bring the primary mirror to a central position. The three elements previously described must be concentric. The two stickers on the mirrors must now be superimposed and centred on the crosshair (see figure 41 B).

When the two mirrors are successfully concentric, and centred in relation to the collimator, we can gently tighten the three collimation screws, one after the other, using small movements. The secondary mirror is now immobilised, correctly positioned and correctly

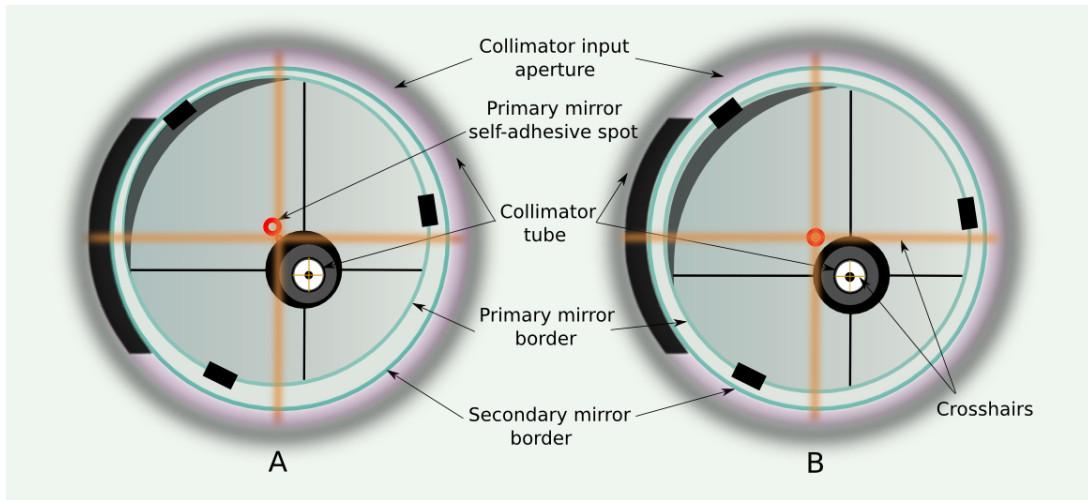


FIGURE 41 – Orientation of the secondary mirror.

oriented.

In this case again, with a little practice everyone can find the right method to carry out this step. With experience, it is possible to completely and correctly adjust the secondary mirror in a single step, without using coloured masks.

6.7 Orientation of the primary mirror.

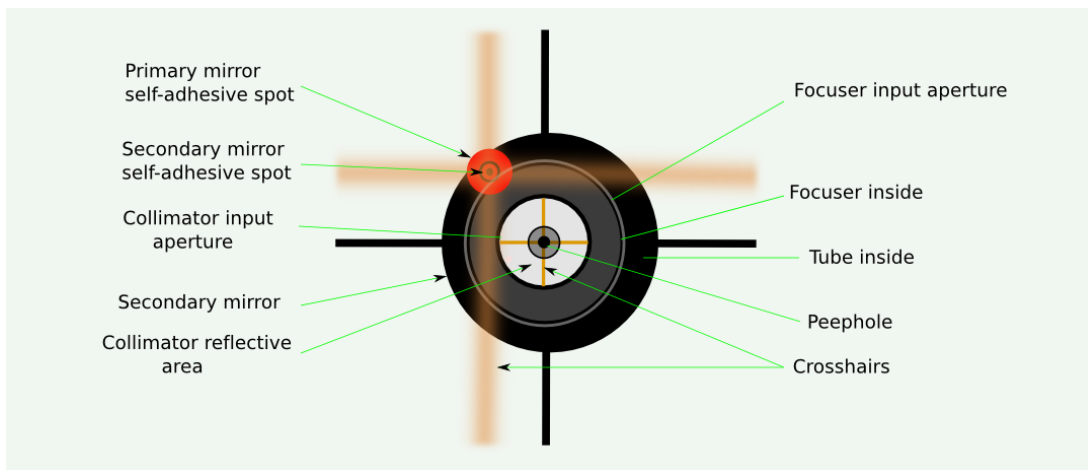


FIGURE 42 – Image of the secondary mirror, reflecting the focuser.

Here, we are going to deal with the three collimation screws of the primary mirror support. Before this, we must first loosen the three lock screws. This step is a fairly easy

compared to the ones we have just dealt with.

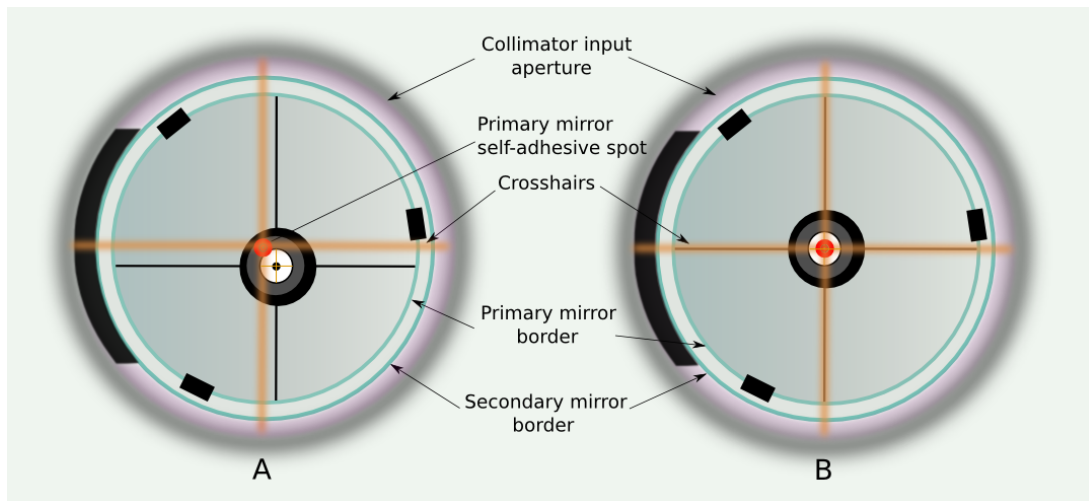


FIGURE 43 – Orientation of the primary mirror.

It is thus our objective to gradually bring the reflection of the secondary mirror into the centre, as indicated in figure 43 B. The secondary mirror itself reflects the image of the focuser seen from the interior of the tube (figure 42). Here we just need to experiment a little with the three collimation screws in order to find out the direction of movement of the reflection of the secondary mirror. This leads us quickly, in a zigzag fashion, to the correct centring.

The collection of elements is now centred, apart from the reflection of the secondary mirror if we have taken the offset into account. In this case, the secondary mirror seems slightly unbalanced towards the primary mirror (towards the right, in the drawing). In order to avoid this effect, we can use the previously mentioned delta mask, which itself must be centred on the tube's axis.

We can now tighten the three lock screws of the primary mirror support, one after the other using small movements. The geometric collimation is now complete. For uniquely visual observation, these adjustments are sufficient.

6.8 Precise collimation on a real star.

The use of a telescope for astrophotography requires a more refined tuning than the previous geometric collimation. The observation of a star at a high magnification enables us to best make this adjustment. The diffraction in the telescope's front aperture and in the edges of its mirrors generates a system of interference. The laws of wave optics, particularly HUYGENS's principle on the propagation of a wave, explain this. The image

of a point source of light is thus not a point, but in fact an Airy disk⁷ with a false central disk surrounded by rings of decreasing luminosity. Figure 44 shows the ideal, theoretical case.

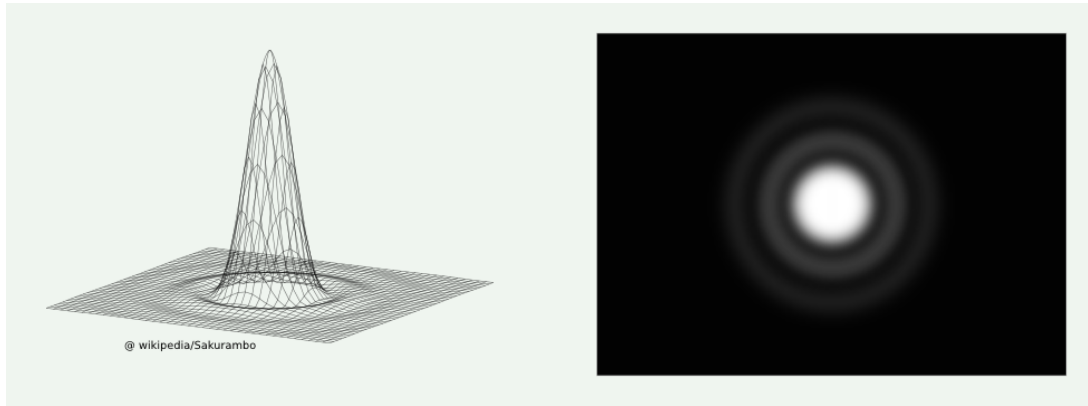


FIGURE 44 – Airy disk.

We would obtain this sort of image of a star only with a perfect optical system, as well as a complete absence of atmospheric turbulence. The limit of a telescope's resolution is its incapacity to differentiate between two very close stars so that the central disks are distinguishable. This is the RAYLEIGH criterion, well known by amateur astronomers, with the following formulae giving the resolution in radians and in seconds of arc. Here, the wavelength is more in the green at 550nm, and D is the primary mirror's diameter.

$$\alpha \text{ in radians} \simeq 1,22 \frac{\lambda}{D}$$

$$\alpha \text{ in seconds} \simeq \frac{120}{D_{mm}}$$

and the diameter of the central disk in relation to the focal length f :

$$\varnothing_{disque} \text{ in microns} \simeq 2,44 \frac{\lambda_{microns} f_{mm}}{D_{mm}}$$

The approach to take from here on can be resumed : we observe, we observe a bit more, attentively, then we adjust one of the primary mirror's collimation screws, then we observe again after having re-centred the image of the star. We repeat the operation in this way, until the point where we can no longer see any dissymmetry in the image. At a high magnification, the simple act of touching one of the screws can move the image of the star in the field, and so it is necessary to take one's time and to act very carefully.

7. Sir George Biddell Airy, English scientist who described this phenomenon in 1835.

Adjusting the collimation screws here is limited to a fraction of turn, up to one twentieth or one thirtieth of turn or less.

We must also, before beginning, ensure that the telescope is thermally balanced. The air inside the tube must be as stable as possible. To begin with, we will make an adjustment in focussing on a star with a magnitude of 1 or 2, bright but not too bright, and with a magnification of about one times the diameter of the primary mirror in mm. It could be useful or even recommended here, to note how for each of the three collimation screws the image of the star moves in the field when we adjust one in one direction or another. For this, we can imagine a clock, and note for example that the collimation screw no.1, when adjusted clockwise, moves the star image towards 11 o'clock in the field of view (figure 45).

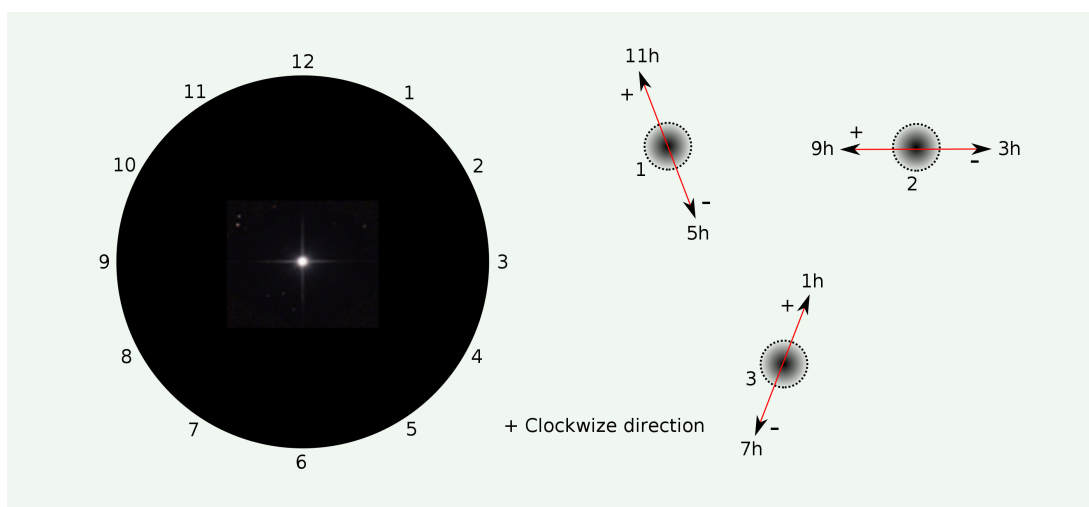


FIGURE 45 – Clock system for the collimation screws of the primary mirror.

This clock system is not superfluous. When we need to adjust one of the collimation screws on a real star at high magnification, it is better to know in advance what will happen when we touch it. This is, after all, reasonable.

We presume here that the telescope is installed on a stable equatorial mount, correctly set up. If this is not the case, at a high magnification the star will drift significantly in the field of view. The images presented here are real, with imperfect optics, atmosphere turbulence and humidity. We are thus in a real-life situation. . . despite this, with a little practice, we should be able to get close to an optimal tuning.

Figure 46 shows an unfocused star, seen in a deliberately badly-adjusted instrument, and with a magnification of one times the diameter of the primary mirror in *mm*. Here, it is a case of showing the three basic operations necessary to decrease the dissymmetry observed. The arrow indicates the direction of the movement to carry out (A), essentially

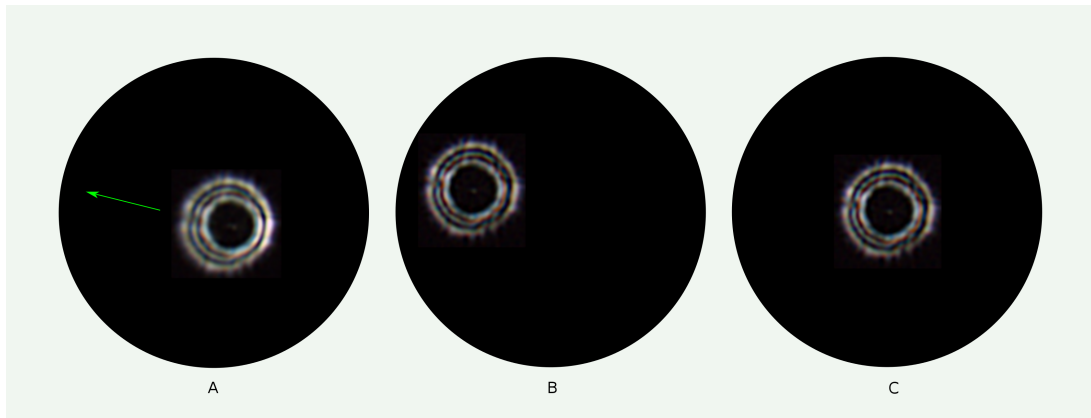


FIGURE 46 – Extra-focal images.

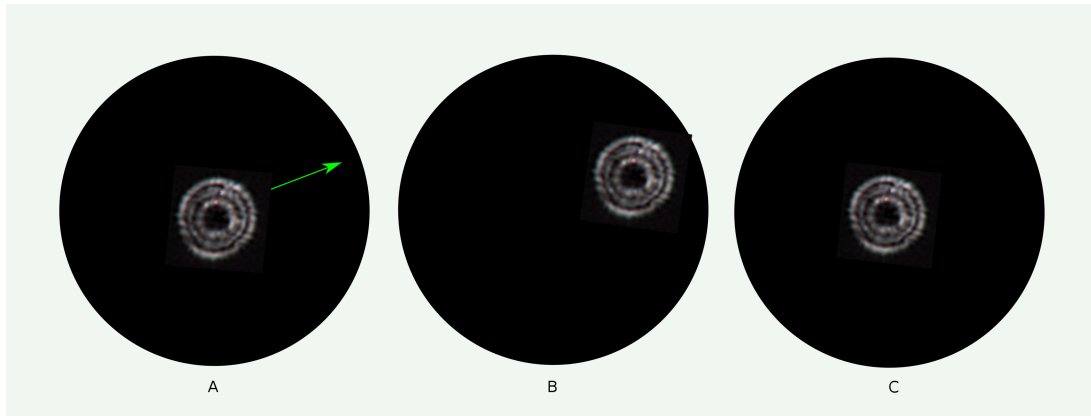


FIGURE 47 – Intra-focal images .

with the collimation screw 2 in a positive direction (B) if we refer to the previously-described clock system. And, finally, the re-centring of the star (C) enables us to verify the result of the action carried out. The final image shows a few defects, as well as a slight dissymmetry. We must make yet another adjustment.

In a similar way, figure 47 represents the same type of correction, but this time intra-focally. The following step consists in doubling the magnification to twice the diameter of the primary mirror in *mm* (figure 48). Here again, we must check to correct the dissymmetry yet visible, with the same method of operating both intra- and extra-focally. A star with a magnitude of 2 or 3 is sufficient for this adjustment.

Finally, to finish, after a precise focus (figure 49), and with an even higher magnification, if possible, we must try, using fractions of a turn on the collimation screws, to refine the image as best as we can (D). With a little luck, and above all very little turbulence,

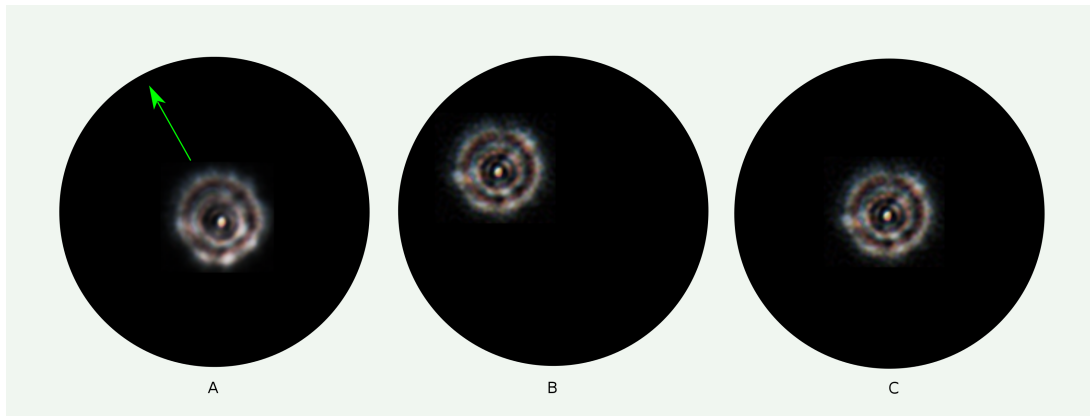


FIGURE 48 – Extra-focal images at a high magnification.

we can hope to see the first ring of an Airy disk.

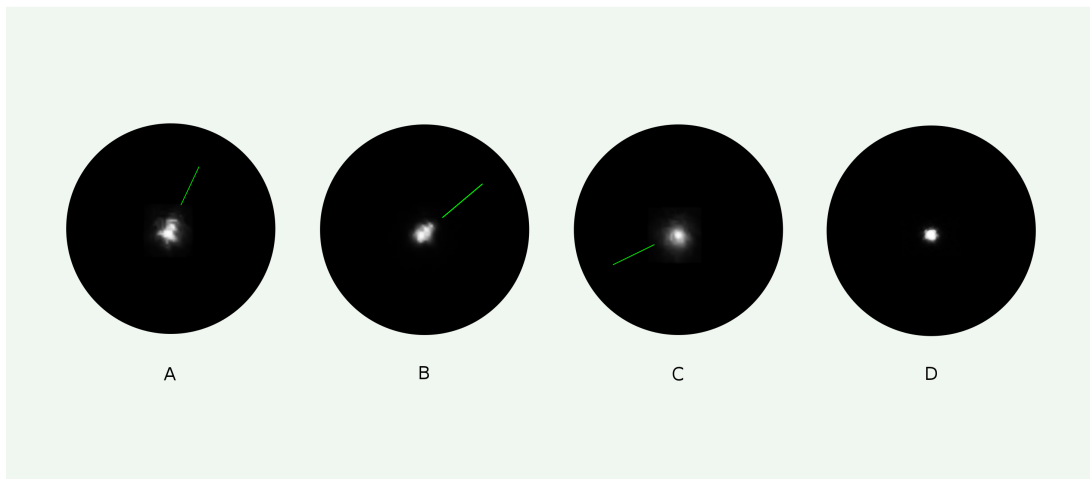


FIGURE 49 – Images focused at a high magnification.

Here concludes this study on Newtonian telescopes. I cannot rule out any imprecision or even error in certain developments, and so corrections will possibly be covered in an updated version of the document.

This document was written with *L^AT_EX* and drawings with *Inkscape*, all under *macOS* and a 21-inch iMac. Special thanks to Natalie Varnier who has translated this document in English.

October 2013 Lionel Fournigault